ISSN: 1863-5598

ZKZ 64717
10–24

Bodo´s Power Systems®

Electronics in Motion and Conversion

October 2024

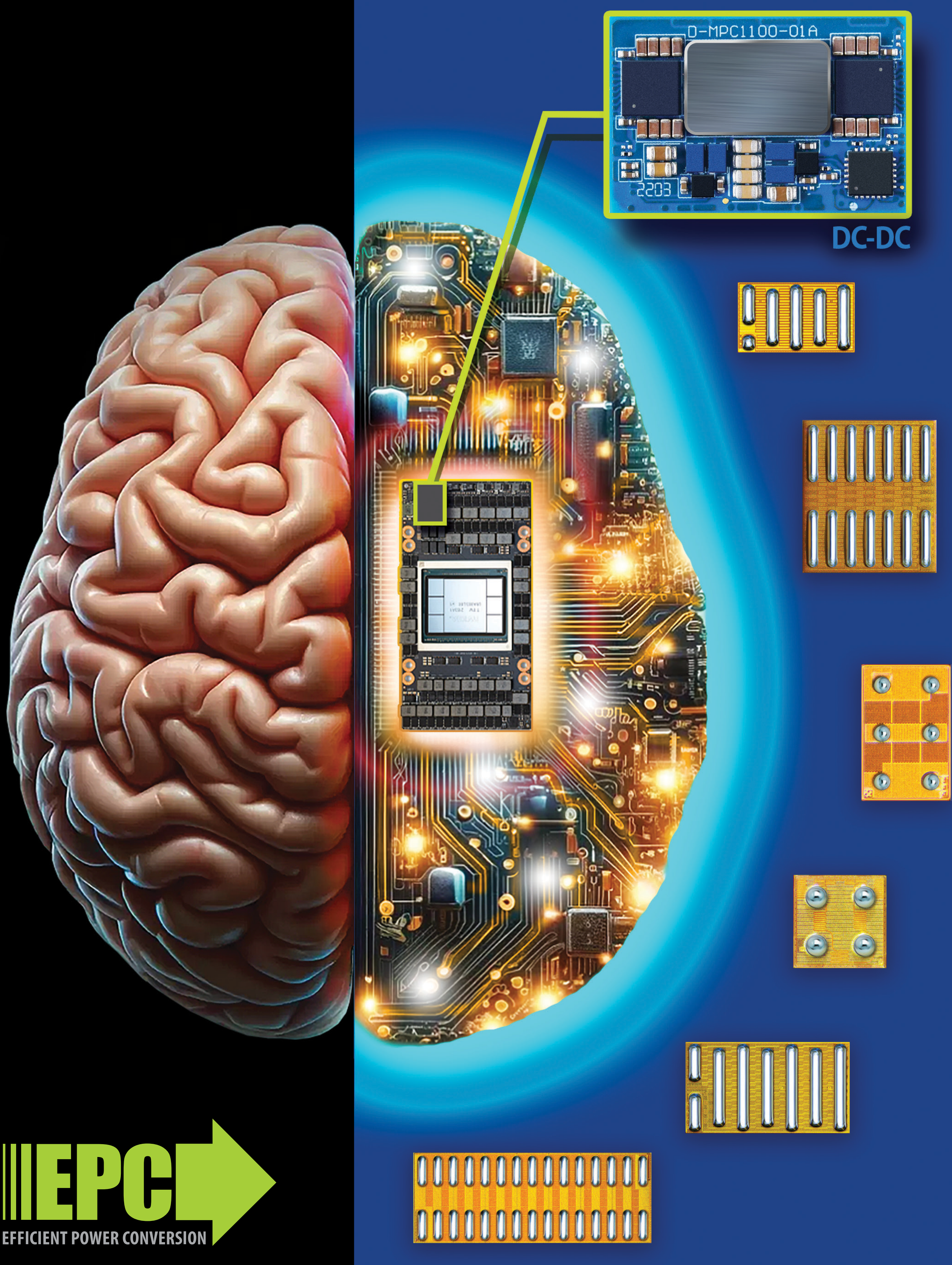

PULSED INDUCTANCE MEASUREMENT

POWER CHOKE TESTER DPG10/20 SERIES

Inductance measurement from 0.1 A to 10 kA

KEY FEATURES

Measurement of the

- **Incremental inductance** $L_{inc}(i)$ and $L_{inc}(\int U dt)$
- **Secant inductance** $L_{sec}(i)$ and $L_{sec}(\int U dt)$
- **Flux linkage** $\psi(i)$
- **Magnetic co-energy** $W_{co}(i)$
- **Flux density** $B(i)$
- **DC resistance**

Also suitable for 3-phase inductors

WIDE RANGE OF MODELS

7 models available with maximum test current from 100A to 10000A and maximum pulse energy from 1350J to 15000J

KEY BENEFITS

- Very **easy and fast** measurement
- **Lightweight, small and affordable price-point** despite of the high measuring current up to 10000A
- **High sample rate and very wide pulse width range** => suitable for all core materials

APPLICATIONS

Suitable for all inductive components from **small SMD inductors** to **very large power reactors in the MVA range**

- **Development, research** and **quality inspection**
- **Routine tests** of small batch series and mass production

Technological leader in pulsed inductance measurement for 18 years

www.ed-k.de

Content

Supporters & Friends

WÜRTH ELEKTRONIK MORE THAN YOU EXPECT

ULTRA LOW LOSSES

WE-MXGI

WE meet @ electronica
Hall A6 - 502

With the WE-MXGI Würth Elektronik offers the newest molded power inductor series. It combines an innovative iron alloy material that provides high permability for lowest R_{DC} values combined with an optimized wire geometry.

Ready to Design-In? Take advantage of personal technical support and free samples ex-stock.
www.we-online.com/WE-MXGI

Highlights
- Extremely high power density
- Ultra low R_{DC} values and AC losses
- Magnetically shielded
- Optimized for high switching frequencies beyond 1 MHz

#UltraLowLosses

A Media
Katzbek 17a
24235 Laboe, Germany
Phone: +49 4343 42 17 90
Fax: +49 4343 42 17 89
info@bodospower.com
www.bodospower.com

Founder
Bodo Arlt, Dipl.-Ing.
bodo@bodospower.com

Editor in Chief
Alfred Vollmer, Dipl.-Ing.
alfred@bodospower.com

Correspondent Editor Bavaria
Roland R. Ackermann
roland@bodospower.com

Editor China
Min Xu – xumin@i2imedia.net

US Support
Rusty Dodge
rusty@eetech.com

Creative Direction & Production
Bianka Gehlert
b.gehlert@t-online.de

Publisher
Holger Moscheik
holger@bodospower.com

Free Subscription to qualified readers
Bodo´s Power Systems is available for the following subscription charges:
Annual charge (12 issues) is
150 € world wide · Single issue is 18 €
subscription@bodospower.com

Printing by:
Westdeutsche Verlags- und Druckerei GmbH; 64546 Mörfelden-Walldorf Germany

Obsolescence or Sustainability?

Our washing machine recently broke down and I was reminded that I am both an editor and an electrical engineer. It was manufactured by a well-known industry-leading company and just a few years old. So, being an engineer, I opened it up and checked the pump because the code on the display indicated that this was the problem. Everything was dry and the tubes, gaskets etc. were in perfect condition. Eventually, I realized that the pump motor was broken, so I ordered a new one - which worked outside the washing machine but not when it was driven by the machine. I checked what I could do without access to the schematics, documentation or an oscilloscope. Finally, I realized that it was the power electronic unit that was broken: a power semiconductor as well as an accompanying device (a diode?) had blown up (the package literally exploded, but as the entire PCB was filled with SMDs, so I was unable to repair it). So, I ordered a new power unit, and the washing machine is in service again.

I found it difficult disposing of an entire and complex board, only because of the failure of two tiny components. Exchanging the pump's motor was fine, and in terms of cost it was just 15 % of the cost of a new washing machine, but the power electronic unit cost another 40 % of the cost of a new washing machine. Whenever a non-engineer encounters such a failure the person has to call the service partner who roughly charges another 20 % of the cost of a new machine for his time. Even for me, this was basically an economic total failure and maybe I should have bought a new machine, which always come with a two-year warranty.

So, basically, the failure of a power semiconductor weighing just one gram turned a 70,000 g machine into scrap metal/concrete/plastic from an economic point of view. This may be good for the economy, but it is a small disaster for the environment. I personally think that we need to find better trade-offs between high-cost pressure and design for repairability in an economic way. With an extra cost of may be two Euros/Dollars on the BOM we might be able to significantly facilitate cheap repairs. If the marketing people could promote this aspect in a positive way, they could probably be able to charge an extra 10 Euros/Dollars more for the machine on the consumer market, even in the extremely competitive market of white goods. However, it would need to be highlighted as a benefit.

Let's continue to talk about such aspects of repairability at Bodo's WBG Event on December 3 and 4 in Munich. At this unique conference, engineers will receive a comprehensive view and insight on today's GaN and SiC solutions. By the way: If you are quick and book your tickets between October 1 and 18 you will receive an extra early bird discount – only on www.bodoswbg.com.

Bodo's magazine is delivered by postal service to all places in the world. It is the only magazine that spreads technical information on power electronics globally. We have EETech as a partner serving our clients in North America. If you speak the language, or just want to have a look, don't miss our Chinese version at bodospowerchina.com. An archive of the magazine with every single issue is available for free at our website bodospower.com.

My Green Power Tip for the Month: Design for repairability! Our environment and our planet with its limited resources will thank you.

Alfred Vollmer

Events

eMove 360° 2024
Munich, Germany October 15 – 17
www.emove360.com

SPCD 2024
Noordwijk, The Netherlands
October 15 – 18
www.spcd.space

ECCE 2024
Phoenix, AZ, USA October 20 – 24
www.ieee-ecce.org

WiPDA 2024
Dayton, OH, USA November 4 – 6
www.wipda.org

electronica 2024
Munich, Germany November 12 – 15
https://electronica.de

SEMICON Europa 2024
Munich, Germany November 12 – 15
www.semiconeuropa.org

sps 2024
Nuremberg, Germany November 12 – 14
https://sps.mesago.com

DMC 2024
Grenoble, France November 18 – 20
https://attend.ieee.org/dmc-2024

Bodo's WBG Event 2024
Munich, Germany December 3 – 4
www.bodoswbg.com

World's first 300 mm Power Gallium Nitride (GaN) Technology

Infineon Technologies has succeeded in developing the world's first 300 mm power gallium nitride (GaN) wafer technology, accomplished in an existing and scalable high-volume manufacturing environment - a "breakthrough" which is said to "help substantially drive the market for GaN-based power semiconductors". Chip production on 300 mm wafers offers 2.3 times more chips per wafer than on 200 mm wafers. "The technological breakthrough will be an industry game-changer and enable us to unlock the full potential of gallium nitride", Jochen Hanebeck, CEO of Infineon Technologies, says. "Infineon is mastering all three relevant materials: silicon, silicon carbide and gallium nitride. Nearly one year after the acquisition of GaN Systems, we are demonstrating again that we are determined to be a leader in the fast-growing GaN market." Infineon has succeeded in manufacturing 300 mm GaN wafers on an integrated pilot line in existing 300 mm silicon production in its power fab in Villach/Austria. The company intends to "further scale GaN capacity aligned with market needs". Infineon claims that "300 mm GaN manufacturing will put Infineon in a position to shape the growing GaN market which is estimated to reach

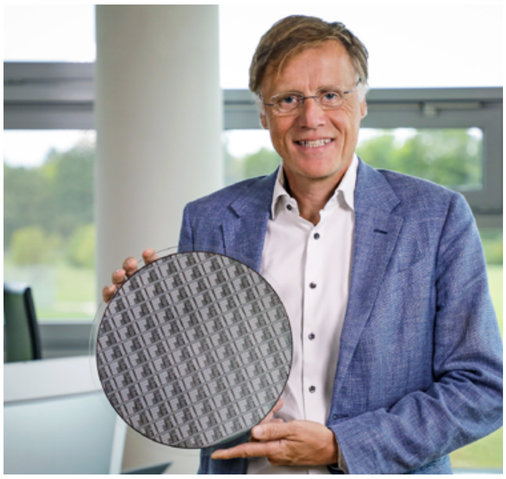

several billion US-Dollars by the end of the decade" and that "fully scaled 300 mm GaN production will contribute to GaN cost parity with silicon on $R_{DS(on)}$ level, which means cost parity for comparable Si and GaN products. The semiconductor manufacturer will present the first 300 mm GaN wafers to the public at the electronica trade show in November 2024 in Munich.

www.infineon.com

electronica 2024: The electronics Trade Show turns 60

electronica celebrated its premiere in 1964 as the first trade fair in Germany devoted solely to electronic components. In the meantime, it has been accompanying innovations in the international electronics industry for six decades, providing a market overview of its latest products, technologies and solutions every two years. In 2024, this trade fair for electronics will celebrate its 60th anniversary from November 12 to 15, occupying all 18 exhibition halls for the first time ever (together with SEMICON Europe in two halls). The focus will be on the future vision of an all electric society. Already at the first edition in Munich in October 1964 a total of 407 companies from 16 countries exhibited on an area of 4,100 square meters, and around 14,000 trade visitors came to visit on the eight days of the fair. Already now the trade show organizer states that the 2024 edition of electronica "will be the biggest electronica of all time".

www.electronica.de

Funding of up to $1.6 Billion in CHIPS and Science Act

Texas Instruments (TI) and the U.S. Department of Commerce have signed a non-binding Preliminary Memorandum of Terms for up to $1.6 billion in proposed direct funding under the CHIPS and Science Act to support three 300 mm wafer fabs already under construction in Texas and Utah. In addition, TI expects to receive an estimated $6 billion to $8 billion from the U.S. Department of Treasury's Investment Tax Credit for qualified U.S. manufacturing investments. The proposed direct funding, coupled with the investment tax credit, would help TI provide a geopolitically dependable supply of essential analog and embedded processing semiconductors. The proposed direct funding under the CHIPS Act would support TI's investment of more than $18 billion through 2029, which is part of the company's broader investment in manufacturing. This proposed direct funding will support three new wafer fabs, two in Sherman, Texas, (SM1 and SM2) and one in Lehi, Utah (LFAB2), specifically to construct and build the SM1 cleanroom and complete pilot line for first production, to construct and build the LFAB2 cleanroom for first production and to construct the SM2 shell. They will produce semiconductors in 28 nm to 130 nm technology nodes.

www.ti.com

Long-Term Supply Agreement for SiC Power Devices signed

ROHM and United Automotive Electronic Systems (UAES), a Tier 1 automotive supplier in China, have recently entered into a long-term supply agreement for SiC power devices. Already since 2015, ROHM and UAES have been collaborating and carrying out detailed technical exchanges on automotive applications utilizing SiC power devices. This partnership deepened in 2020 with the establishment of the SiC Joint Research Institute at the UAES headquarters in Shanghai, China. And in 2021 ROHM's advanced SiC power devices and peripheral components were highly evaluated by UAES, resulting in ROHM being selected as a preferred supplier. The close long-standing technical partnership has led to the production and adoption of numerous automotive products equipped with ROHM SiCs, such as onboard chargers and inverters for electric vehicles. This long-term supply agreement is said to ensure UAES sufficient access to SiC power devices to meet the growing demand for SiC-based inverter modules. Going forward, both companies will deepen their collaboration, contributing to technological innovation in the automotive sector by accelerating the development of SiC power solutions for EVs.

www.rohm.com

Investment in additional R&D Capabilities in Europe and Asia

To satisfy the growing global demand for current and voltage sensing driven by the push towards decarbonization and greater electrification, LEM has opened new research and development facilities in Munich and Shanghai. The two sites are said to enable LEM to build greater intelligence into its sensors and to have development bases closer to key customers, while also promoting deeper collaboration on projects and the efficient sharing of vital product design information. While the China site will be kitted out with the very latest laboratory equipment, the site in Germany will focus on ASIC design and semiconductor technology that will help accelerate LEM's innovation in integrated current sensors (ICSs). This latest investment in additional R&D facilities in Europe and Asia follows on from LEM's recent inauguration of a factory in Malaysia. LEM's investment in the state of Penang was an acknowledgment of the region's expertise in ASIC technology and its specialization in semiconductor design and production. There are already 10 employees in place at Munich and this number will increase in line with LEM's growth plans for the site. At the 1400 m² Shanghai facility, there are currently 30 staff with the capacity to more than double that number in the future, many of whom will be involved in R&D.

www.lem.com

PCIM Asia 2024 grew significantly

PCIM Asia 2024, an international platform for communication and exchange in power electronics, intelligent motion, renewable energy and energy management, successfully concluded late August at the Shenzhen World Exhibition and Convention Center in China. Setting new records across nearly all metrics, the 2024 edition was the largest and most comprehensive iteration of the event to date. Floor space grew by 8,000 m² (+67 %) to a total of 20,000 m². The number of visitors (from 41 countries) increased 20 % over the 2023 edition to a total of 18,346, while the number of exhibitors (from 13 countries and regions) increased 28 % over the 2023 edition to a total of 232. To promote further dialogue and collaboration, the exhibition presented a series of industry forums, exhibitor forums and round-table discussions, covering topics ranging from wide-bandgap semiconductors and e-mobility to eVTOL development. At these sessions, representatives from several companies and researchers shared insights on development trends, new market applications and cutting-edge research. Alongside the exhibition, the PCIM Asia Conference 2024 once again featured technical advancements and applications in power electronics. 981 conference visitors listened to 3 keynote speeches, 12 oral sessions and 6 poster sessions as well as to 104 presentations.

PCIM Asia is jointly organised by Guangzhou Guangya Messe Frankfurt Co Ltd and Mesago Messe Frankfurt GmbH. The next edition will take place from 14 – 16 August 2025 at the Shanghai New International Expo Centre (SNIEC) in Shanghai, China.

www.pcimasia-expo.com

Acquisition of Austrian Power Supply Company

RECOM has enhanced its portfolio of products and capabilities by acquiring Leco. Like RECOM Leco is based in Austria, and according to RECOM Leco "is one of only a few companies that specialize in design and manufacture of full custom, high-end power solutions". By integrating LECO's engineering expertise and high-end power conversion products into its portfolio, RECOM enhances its market position and delivers more, comprehensive, high-end power supply solutions to its global customer base. "We are proud to have established this partnership with LECO. This provides us with an opportunity to expand our engineering capabilities and product portfolio for our customers, especially in industrial, automation & supply chain end-markets, as well as leveraging our global footprint for the sale of LECO high-end products.", Karsten Bier, CEO and Shareholder, RECOM.

www.recom-power.com

Current Sensors achieve ASIL C(D) Compliance

Melexis reaches ASIL C safety compliance with its smart IVT (current, voltage, temperature) sensing platform. The Hall-effect MLX91230 and Shunt interface MLX91231 simplify the achievement of ISO 26262 ASIL C(D) architecture for critical vehicle functions such as battery management systems (BMS), smart pyrofuses, and high-voltage charging systems. Both devices integrate a wide range of smart functionality, including the microcontroller unit (MCU) with on-board flash memory that supports custom software deployment and extensive compensation of system imperfections. The diagnosable OCD allows for direct input to the Pyro-Fuse driver, enabling the simple deployment of smart pyrofuses with fewer components. Furthermore, the ASIL C safety level applies to the current sensing function and OCD, as well as the additional temperature and voltage measurement channels. The selectable LIN or UART output enables integration with 12V battery applications and power distribution modules, as well as direct communication with BMS or UART-over-CAN.

www.melexis.com

Executive Vice President for German Electronics Specialist

With effect from 1 August 2024 Thomas Garz has been appointed Executive Vice President for the Würth Elektronik eiSos Group. The 37-year-old has been with the Würth Group since 2006. Most recently, he was Senior Vice President of the Würth Line Craft, the core business of the Würth Group, for Scandinavia and additionally responsible for International Systems of the Würth Line. The organizational structure of the Würth Elektronik eiSos Group will remain unchanged as a result of this appointment. Before taking up his position as the Senior Vice President of the Würth Line Craft for Scandinavia, Thomas Garz held various positions, including sales and shop manager, assistant to the management and auditor for Würth.

www.we-online.com

Waves of Innovation

AVL, Wolfspeed, and DEIF are pioneering the transformation of marine mobility towards a zero-carbon emission future and came together for a panel discussion during the SMM (Shipbuilding, Machinery & Marine Technology trade fair) which recently took place in Hamburg.

Here, they discussed the benefits of the energy efficiency achieved using power converters based on silicon carbide MOSFET devices (SiC converters) compared to traditional converters using silicon IGBT devices (Si converters). System level analysis, for example, shows an estimated total efficiency improvement from 93% to 96% in marine applications. These types of breakthrough innovations in maritime mobility can significantly reduce CO_2 emissions as the world continues to drive towards a more sustainable future.

Expert panelists, at the *Historischer Speicherboden* included:
- Guy Moxey, Vice President, Power, Wolfspeed
- Paul Wheeler, Vice President and GM, Power Modules, Wolfspeed
- Erwin Reisinger, Chief Engineer, Electrification, AVL
- Christian Nielsen, Group CEO, DEIF

www.wolfspeed.com
www.avl.com
www.deif.de

Industrialized process for pre-pasted Thermal Interface Material (TIM)

FEATURES

- Optimized for Fuji modules
- Increased lifetime of IGBT
- Advanced IGBT power density

- Thermal – Benefits
  - Higher thermal conductivity
  - Uniform thermal resistance
  - Increased reliability and lifetime

- Process – Benefits
  - Outsourcing of a “dirty” process
  - Stable quality level
  - Computer controlled automated process
  - Increased System reliability
  - Printing according customer specification
  - TIM upon customers preference possible

New Semiconductor Material: AlYN promises more Energy-Efficiency

Researchers at Fraunhofer IAF (Fraunhofer Institute for Applied Solid State Physics) have reported that they "made a breakthrough in the field of semiconductor materials": With Aluminum Yttrium Nitride (AlYN), they have succeeded in fabricating and characterizing a new and promising semiconductor material using the MOCVD process. Due to its excellent material properties and its adaptability to gallium nitride (GaN), AlYN is said to have "enormous potential for use in energy-efficient high-frequency and high-performance electronics for information and communications technology". AlYN shows outstanding material properties, however, the growth of the material has been a major challenge. Until now, AlYN could only be deposited by magnetron sputtering. Researchers at Fraunhofer IAF have now succeeded in fabricating the new material using metal-organic chemical vapor deposition (MOCVD) technology, thus enabling the development of new, diverse applications. The institute thinks that "with its promising material properties, AlYN could become a key material for future technological innovations". Recent research had already demonstrated the material properties of AlYN, such as ferroelectricity. In developing the new compound semiconductor, the researchers at Fraunhofer IAF focused primarily on its adaptability to gallium nitride (GaN) – especially in terms of the lattice structure.

www.iaf.fraunhofer.de

Joining the Global Battery Alliance

Siemens Digital Industries Software announced it has joined the Global Battery Alliance (GBA), a collaboration platform that brings together international organizations, NGOs, industry actors, academics and multiple governments to align collectively in a pre-competitive approach, to drive systemic change along the entire battery manufacturing value chain. The vision of the GBA is to achieve three fundamental outcomes, which Siemens endorses and actively contributes to: establish a circular battery value chain, establish a low carbon economy in the value chain, and safeguard human rights and economic development. Through dedication to these principles, Siemens aims to bring about sustainable practices within the battery industry that not only minimize environmental impact but also create new job opportunities and generate additional economic value for communities worldwide. By joining GBA, Siemens is aligning with major stakeholders across the entire battery supply chain, spanning from material developers to cell suppliers, OEMs, and government bodies to strive towards a greener and more ethical future.

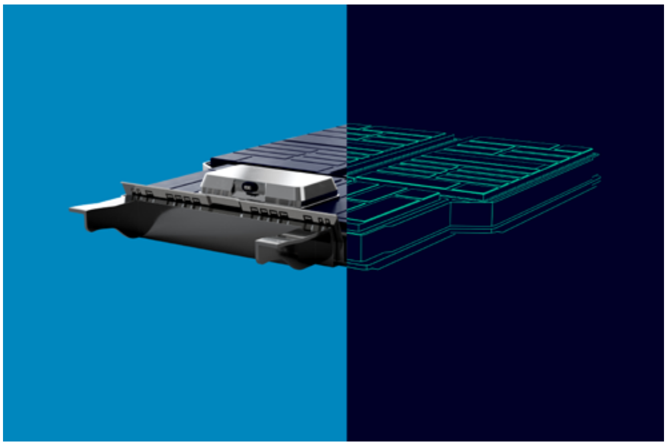

https://xcelerator.siemens.com

65 W USB-C design with 30 % lower Temperatures and 96 % Efficiency

Pulsiv has introduced a reference design which is claimed to be "the world's most efficient 65 W USB-C GaN optimised reference design developed to address the complex challenges associated with thermal performance in power supplies". According to Dr. Tim Moore, Chief Product Officer at Pulsiv, "this development is set to revolutionize the USB-C fast charging space by offering a unique combination of features and benefits not seen in other designs". This is high praise at the beginning, so let's have a closer look at the design.

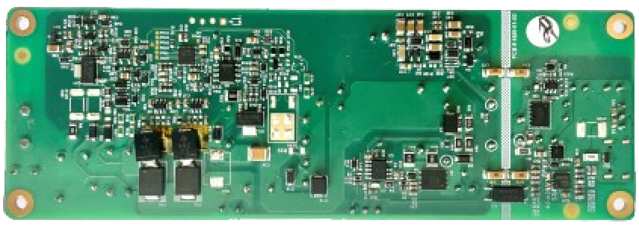

The PSV-RDAD-65USB reference design combines Pulsiv OSMIUM technology with an industry standard QR flyback and highly optimized, ultra-compact magnetics. It represents the first in a series of designs aimed at pushing the boundaries of power conversion by "drastically lowering operating temperatures, minimizing losses, and reducing size to create a sustainable platform for the USB-C standard", says Tim Moore.

Operating from an input voltage range of 90 – 265 V_{AC} without input voltage derating the design provides DC voltages between 5 and 20 V at the output while supporting PD3.0, QC4.0, BC1.2 and PPS for fast charging at a maximum output power of 65 W. The transformer temperature is said to be 30.3 degrees above the ambient temperature. Working with an operating frequency of 125 kHz the designs enables a peak efficiency of 96 %, however, the average efficiency is specified to be 95 %. This is enabled by the quasi-resonant (QR) flyback DC/DC converter which Tim Moore calls "GaN optimized". Maximum line currents are 0.5 A, and inrush currents are eliminated.

The Pulsiv OSMIUM reference design demonstrates "a significant improvement in thermal performance and reduces critical component temperatures by more than 30% compared to other designs", claims Tim Moore, who has been managing the development of this design. At full load with 230 V_{AC} at the input and at an ambient temperature of 26.1 °C, the flyback transformer's temperature is said to be 33.9 degrees higher than the ambient temperature; at 265 V it is said to be 30.3 degrees higher. Therefore, for Tim Moore it "is likely to set a new benchmark and enables 65 W fast charging in space constrained environments and/or heat sensitive applications such as in-wall plug sockets that incorporate USB-C connectivity".

Using a half-active bridge design

Pulsiv OSMIUM technology senses AC line voltage and frequency to adjust capacitor charging time; therefore the circuit draws no line current at the AC zero voltage crossing. This enables a simple half-active bridge implementation to increase efficiency, especially at low line conditions. MOSFETs in the lower half of the AC-to-DC bridge are carefully controlled, in combination with high-side diodes. The half-active bridge in this design strikes the delicate balance between efficiency, cost, and complexity and supports universal input with efficiency gains of 0.7 % at full load from a 115 V_{AC} supply.

Smaller transformer and GaN transistors

The HVDC output generated varies between the peak AC input and 150 V to drive the QR flyback at maximum efficiency. The wider voltage range significantly reduces primary side inductance to enable the use of an EQ20 transformer which was developed in partnership with the magnetics company Frenetic. Compared to an RM8 core typically used in other designs this results in a 20 % size reduction and 50 % efficiency improvement. GaN transistors from Innoscience have lowered the R_{DSon} and parasitic capacitance to reduce losses in both the flyback and synchronous rectifier sub-systems.

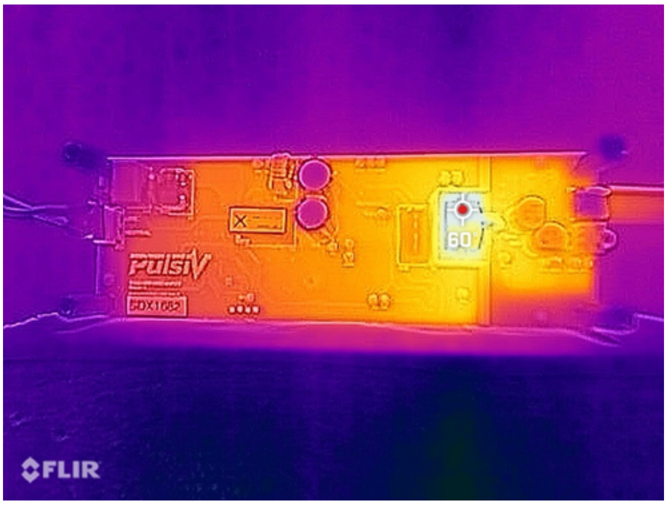

Heat scan of the PSV-EBAD-65USB evaluation board:
V_{in} = 230 V_{AC}; V_{out} = 20 V; I_{out} = 3.25 A;
ambient temperature = 26.1 °C

The PSV-RDAD-65USB document package is available to download free from the Pulsiv website and includes a datasheet, schematics, bill of materials and Altium files. A PSV-EBAD-65USB evaluation board is available for sale.

Learn more:
https://www.pulsiv.com/power-supply-technology-all-reference-designs/reference-designs-full-ac-dc-power-supplies/psv-rdad-65usb

www.pulsiv.com

Silicon Carbide Module Solution to Boost Clean Energy Capacity

2300V modules utilize 200mm silicon carbide technology to deliver energy efficiency for various applications, including renewable energy, energy storage, and high-capacity fast-charging infrastructure

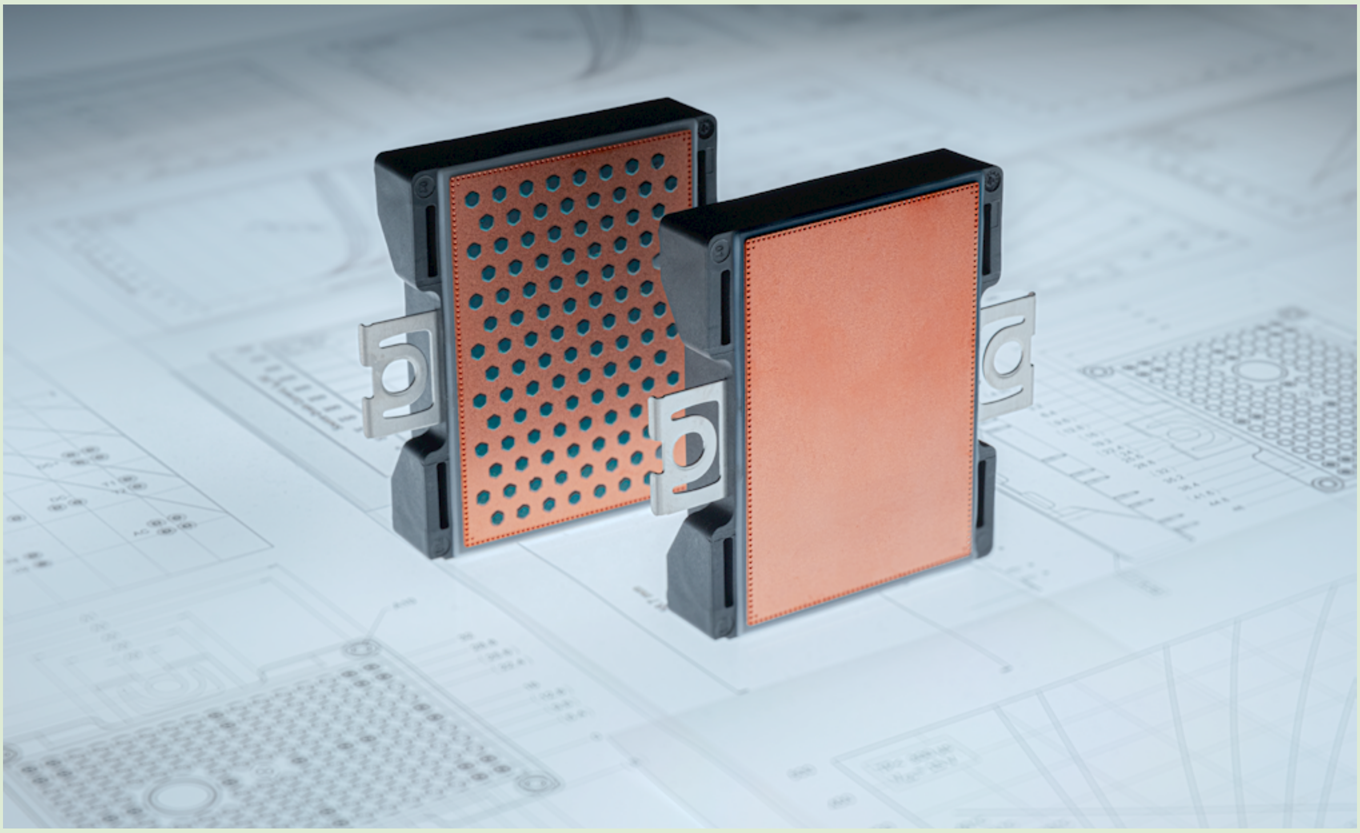

The 2300V baseplate-less silicon carbide power modules for 1500V DC Bus applications were developed and launched utilizing Wolfspeed's state-of-the-art 200mm silicon carbide wafers

Wolfspeed unveiled a silicon carbide module designed to transform the renewable energy, energy storage, and high-capacity fast-charging sectors through improved efficiency, durability, reliability, and scalability. The 2300V baseplate-less silicon carbide power modules for 1500V DC Bus applications were developed and launched utilizing Wolfspeed's state-of-the-art 200mm silicon carbide wafers.

Wolfspeed's 2300V modules will improve system efficiency, while reducing the number of passive components. They offer 15% greater voltage headroom compared to similar silicon carbide modules, improved dynamic performance with consistent temperature stability, and a substantial reduction in EMI filter size. Wolfspeed's technology achieves a 77% reduction in switching losses over IGBTs and a 2-3x reduction in switching losses for silicon carbide devices intended for 1500V applications. 2300V silicon carbide modules will allow system designers to leverage lower cost printed circuit boards to cut manufacturing costs and significantly reduce development time compared to legacy bus bar solutions. Furthermore, Wolfspeed's 2300V modules will enable the industry to adopt the two-level topology, resulting in simplified system design and reduced driver count compared to IGBT-based three-level configurations. The benefits of 2300V modules support a building block approach to easily scale power tenfold, from kilowatts to megawatts. The 2300V silicon carbide modules will allow customers to further enhance the lifetime and durability of their systems. This is achieved through an optimized Failure in Time rate for continuous 1500V DC operation and improved cosmic ray susceptibility compared to a 2000V design. When used in a two-level implementation, 2300V modules reduce the amount of potential single points of failure across the system.

www.wolfspeed.com


"Meet the TOP EXPERTS
for SiC and GaN!"
Secure your Early Bird ticket by October 18!
bodoswbg.com/register
Bodo's
Wide Bandgap
EVENT 2024
December 3-4
Hilton Munich Airport
Mark your Calendar!
Day 1
Opening Roundtable
& Come Together
Day 2
Conference
& Tabletop Exhibition
bodoswbg.com
Bodo´s Power Systems®

Why knowing the Product Carbon Footprint is important

An environmental-conscious semiconductor manufacturer needs to provide more than "just" products to enable greener solutions. Dr. Peter Wawer, Division President Green Industrial Power (GIP) at Infineon, explains, why the Product Carbon Footprint (PCF) is of high importance and how design engineers can benefit from knowing the PCF.

By Alfred Vollmer, Bodo's Power Systems

Dr. Peter Wawer, Division President Green Industrial Power (GIP) at Infineon.

Alfred: What does Product Carbon Footprint exactly mean?

Peter: Infineon's Product Carbon Footprint sets a new level of transparency, enabling customers to increase transparency on their own carbon footprint and supply chain. By revealing our PCF metrics, we're extending the visibility of our CO_2 emissions reduction efforts, providing transparency from our corporate actions down to the individual product level.

Why does Infineon provide Product Carbon Footprint information about its products?

As a leader in sustainability, we are driving the vision of a net-zero society and empowering our customers for own product carbon footprint calculations and their decarbonization efforts. We are taking a leading role in carbon transparency to reduce carbon emissions even more effectively.

This is another step in Infineon's journey to drive decarbonization and digitalization together with customers and partners. Moreover, the effort supports informed decision making for customers to leverage additional potential for reducing emissions along the value chain, and hence supports our customers in advancing their own sustainability goals. With the PCF, customers gain deeper insights into their carbon footprint, fostering more effective strategies for their own CO_2 emissions reduction.

For which products do you provide PCF information?

The Product Carbon Footprint covers scope 1 and 2 emissions as well as scope 3 emissions from suppliers and manufacturing partners, all the way to the customer's gate. Detailed information for 17 representative products from Infineon's wide portfolio is freely available at www.infineon.com/pcf. Furthermore, we provide PCF data for about half of our portfolio already now on customer request, with the clear commitment to address the whole product portfolio as soon as possible.

What is the methodology behind the Product Carbon Footprint?

There is no industry standard for PCF calculations available yet. That's why we have developed our own robust methodology to allocate the carbon footprint. It is based on international standards like the Greenhouse Gas Protocol and ISO 14067 to provide a most accurate and comparable picture including all relevant emissions from raw material supply, own production, energy and transportation. The Product Carbon Footprint covers scope 1 and 2 emissions as well as scope 3 emissions from suppliers and manufacturing partners, all the way to the customer's gate.

You talk about PCF. Does Infineon also offer data for a full Life-Cycle-Assessment?

Infineon reports the PCF "from cradle to gate", meaning from raw material extraction, manufacturing and internal transportation to the gate of the customer, as this is the part of the lifecycle of a product that we have most accurate data on. The PCF data Infineon provides to its customers includes detailed information on the manufacturing process, transport, and material level. Influence factors include weight, chip size, number of layers, and material used. So, the PCF covers scope 1 and scope 2 emissions (direct emissions), but also scope 3 upstream emissions from our suppliers and manufacturing partners. The use and recycling phase is harder to determine for Infineon as both depend on the specific use case of the end product that is utilizing our components, the recycling path

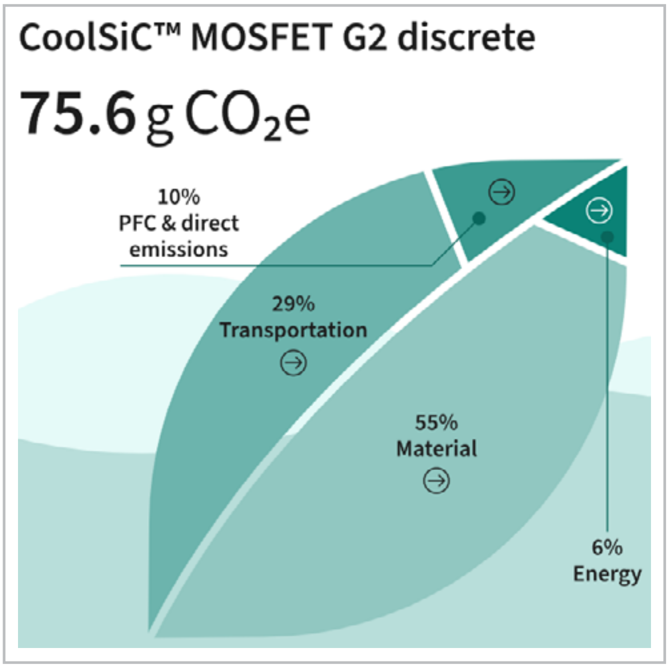

A discrete component of Infineon's CoolSiC MOSFETs Generation 2 family produces 75.6 g of CO_2 emissions reflecting transportation, direct emissions, material, and energy consumed to manufacture the device.

etc. and we do not have clear visibility into this part of the lifecycle. In other words, we are lacking reliable data to calculate a credible full Life-Cycle-Assessment (LCA).

What is Infineon's strategy in terms of carbon neutrality?

Infineon's climate strategy is founded on two pillars: continuous reduction of its own emissions and the active contribution Infineon and its products and solutions make to climate protection thanks to better resource management. Energy efficiency, intelligent PFC abatement concepts and hence reducing CO_2 emissions have long been core elements of Infineon's business model.

The PCF advancement not only propels our decarbonization efforts through adequate solutions but also compliments our earlier pledge to achieve carbon neutrality by 2030 for direct emissions (scopes 1 and 2) and our commitment to set a science-based target encompassing supply chain emissions (scope 3).

Overall, Infineon's products deliver a 34 times ecological net-benefit, that is in total more than 110 million tons of CO_2 equivalents. In other words, the emission savings of our products achieved during their lifetime is estimated to be 34-times higher than the emissions needed for their production.

Which benefit does carbon neutrality offer to the design engineers, the products they work on and their companies?

By revealing our PCF metrics, we're extending the visibility of our CO_2 emissions reduction efforts, demonstrating transparency from our corporate actions down to the individual product level. This enables our customers to gain deeper insights into their carbon footprint, fostering more effective strategies for their own CO_2 emissions reduction and enable conscious purchasing decisions. Infineon is one of the first semiconductor suppliers to deliver such a level of detail to its customers, enabling them to take educated decisions along the value chain.

Achieving carbon neutrality is not an easy task. Where should companies get started, and how should they proceed?

Making life greener should be part of every company's mission; it is paramount for all industries. We want to make an active contribution to global CO_2 reduction and to the implementation of the targets set out in the Paris Climate Agreement.

Infineon's approach is as follows: Avoiding direct emissions and further reducing energy consumption. Purchasing green electricity with guarantees of origin for unavoidable emissions. Compensate the smallest part by certificates that combine development support and CO_2 reduction.

Which role does power electronics play in achieving carbon neutrality?

Continuous improvement of power semiconductors and systems helps to reduce losses and therefore improves the overall efficiency of the system – in other words: less electrical energy is being turned into heat and wasted. To give you an example, Infineon helps to make solar inverters smaller, lighter and more powerful getting more out of photovoltaic with advanced semiconductors based on materials like silicon carbide (SiC) for example. Our devices help to convert direct current (DC) produced by solar panels into alternating current (AC) that can be fed into a public grid or used in industrial, consumer, and mobility applications – with highest efficiency and less conversion losses. Hence Infineon's CoolSiC™ MOSFETs allow for higher currents and reduced heat loss, enabling higher power density and smaller form factors for inverters.

www.Infineon.com

The Role of Gallium Nitride Power Transistors and Integrated Circuits in the Emerging Humanoid Robot Market

The world is entering a new era of automation, where robots are becoming increasingly sophisticated, capable of performing tasks once considered the exclusive domain of humans. At the forefront of this transformation are humanoid robots, designed to mimic the form and functions of the human body.

By Alex Lidow, Ph.D., CEO of Efficient Power Conversion Corporation (EPC)

The Evolution of Humanoid Robots and the Need for Advanced Electronics

These robots are not merely machines; they are complex systems requiring advanced power electronics to operate efficiently and effectively.

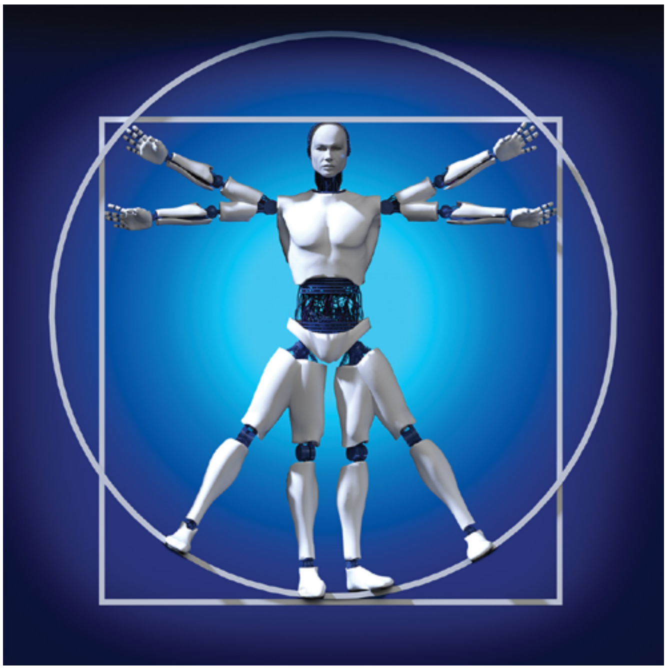

The global humanoid robot market is poised for significant growth over the next several years. As our society ages and birth rates decline, particularly in developed countries, the need for automated labor is becoming more pressing. Humanoid robots are emerging as a viable solution to address labor shortages across various sectors, from healthcare and elderly care to manufacturing and service industries.

However, the widespread adoption of humanoid robots is currently limited by factors such as cost, functional speed, the expense of programming and teaching these robots, and their ability to adapt to unforeseen situations. The pace at which these challenges are overcome will determine the speed at which humanoid robots are deployed across various industries. Ultimately, the success of these advancements depends on society's readiness to integrate robots into daily life and work environments.

Several technological trends are driving the development of humanoid robots, with cost and functionality being the most significant. Advanced power electronics that offer high efficiency, compact size, and reliability are central to these advancements. This is where gallium nitride (GaN) power transistors and integrated circuits (ICs) come into play.

The Mechanical and Sensory Functions of Humanoid Robots

Motor Control: The Heart of Robotic Movement

At the core of any humanoid robot is its ability to move in a manner that closely resembles human movement. This is achieved using brushless DC (BLDC) motors, responsible for driving the robot's joints, limbs, and other mechanical components. A typical humanoid robot is equipped with approximately 40 BLDC motors, each powering different parts of the robot, such as the fingers, toes, arms, legs, neck, and torso.

These motors vary in their power requirements depending on the specific function they perform. For example, the motors driving the robot's fingers may require only a few amperes of current, while those powering the hips or legs may need 80 amperes or more. Regardless of the power requirement, the motors must operate with high efficiency to minimize energy consumption and heat generation, which are critical factors in maintaining the robot's overall performance and reliability.

The Importance of GaN in Motor Control

GaN devices are particularly well-suited for motor control applications within humanoid robots due to their superior electrical properties compared to traditional silicon-based MOSFETs. One of the key advantages of GaN devices is their extremely fast switching speed, which is 10 to 100 times faster than that of silicon MOSFETs. This high-speed switching capability enables the motors to operate at higher frequencies, reducing motor losses and improving overall system efficiency.

The high switching speed of GaN devices also allows for the use of smaller, more reliable ceramic capacitors in place of bulky electrolytic capacitors. This is particularly important in applications where space is at a premium, such as in the motor drives of humanoid robots. By reducing the size of the capacitors, the overall size and weight of the motor drive can be minimized, making it easier to integrate the drive within the motor housing.

Another critical advantage of GaN devices is their lack of reverse recovery charge (Q_{RR}). In silicon-based MOSFETs, the reverse recovery charge can cause significant energy losses during each switching cycle, reducing efficiency and generating additional heat. The absence of Q_{RR} in GaN devices eliminates this energy loss, allowing the motor to operate more efficiently with less heat generation.

Erik Rehmann, GVA expert for Quality Management

gva-power.de

„WHERE INNOVATION GOES IN SERIES: GVA"

Our Development, Production and Quality departments are separated by one floor and two flights of stairs – nothing else. Because all GVA experts share the same systemic understanding and the latest know-how. That´s why we are able to mass-produce innovative developments in the shortest possible time. With guaranteed quality – and gladly also for you!

Your GVA expert:
Jürgen Kolasinski
+49 (0)621 / 78992-22
j.kolasinski@gva-power.de

GVA
POWER ELECTRONICS EXPERTS

Furthermore, the elimination of reverse recovery charge means that less deadtime is required in each switching cycle. Deadtime reduces the amount of power delivered to the motor and can cause acoustic noise. By minimizing deadtime from several hundred nanoseconds to just a few nanoseconds, GaN devices increase the torque per ampere, resulting in more efficient motor operation and a quieter system.

Overall, the use of GaN devices in motor control applications offers significant benefits, including improved efficiency, reduced size and weight, lower cost, and increased reliability. These advantages make GaN the ideal choice for powering the motors in humanoid robots, which require compact, efficient, and reliable power electronics to operate effectively.

GaN Monolithic Power Stages for Motor Drives

One of the most significant advancements in GaN technology is the development of monolithic power stages, such as the EPC23102. These monolithic GaN ICs integrate multiple functions into a single chip, including the power transistor, gate driver, and protection circuitry. The block diagram of the EPC23102 is shown in Figure 1. By integrating key functions into a single chip, the EPC23102 saves valuable design time and space, which are critical factors in the compact and complex environment of a humanoid robot.

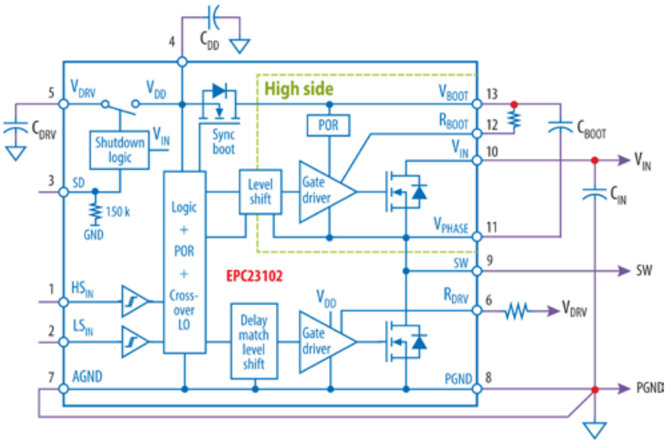

Figure 1: Block diagram of EPC23102 ePower Stage IC

An example of a GaN-based motor drive using the EPC23102 monolithic IC is the EPC9176 reference design, whose block diagram is shown in Figure 2. The EPC9176 is a 400 W motor drive inverter using three EPC23102 integrated circuits with a wide input voltage range of 14 V to 85 V. It can deliver up to 20 A_{RMS} current to the motor, making it suitable for powering most of the robot's smaller joints and actuators.

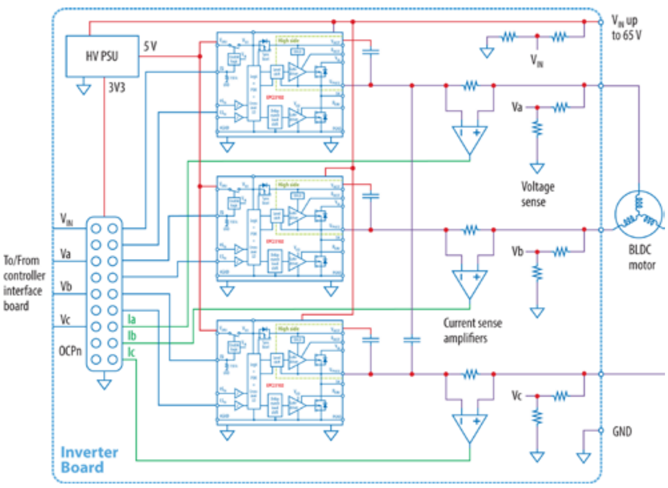

Figure 2: Block diagram of EPC9176 reference design board

Enhancing Robotic Vision: GaN in Lidar Systems

The Role of Lidar in Humanoid Robots

In addition to movement, humanoid robots need to perceive and interact with their environment in a manner like humans. Vision is one of the most critical sensory functions for a humanoid robot, enabling it to navigate its surroundings, avoid obstacles, and perform complex tasks. To achieve this, robots rely on advanced vision systems such as Lidar (Light Detection and Ranging).

Lidar works by emitting laser pulses and measuring the time it takes for the pulses to reflect off objects and return to the sensor. By calculating the time-of-flight of these pulses, lidar systems can create a high-resolution, three-dimensional digital map of the robot's surroundings. In contrast to a map made from camera images, this map provides precise X, Y, and Z coordinates for the entire surroundings, which can then be efficiently processed by the robot's AI to develop spatial awareness and make real-time decisions.

Lidar is particularly well-suited for humanoid robots because it offers high resolution, long-range detection, and fast frame refresh rates, all of which are essential for tasks that require precise and timely information about the environment. However, to maximize the performance of lidar systems, the underlying electronics must be capable of operating at extremely high speeds and with high current density—requirements that are ideally met by GaN devices.

The Advantages of GaN in Lidar Systems

GaN technology has been a critical enabler of lidar systems for over a decade, particularly in applications such as autonomous vehicles and advanced driver-assistance systems (ADAS). The same properties that make GaN ideal for automotive lidar are equally beneficial in humanoid robots.

One of the primary reasons for GaN's dominance in lidar systems is its exceptional switching speed, which is essential for achieving high resolution and fast frame refresh rates. GaN devices can switch at speeds that are 100 times faster than silicon MOSFETs, allowing the lidar system to emit and detect laser pulses at a much higher frequency. This increased frequency translates directly into higher resolution, enabling the robot to create more detailed and accurate maps of its surroundings.

In addition to speed, GaN devices offer a higher current density than silicon, allowing for more powerful laser pulses. This is particularly important for long-range detection, where the laser pulses need to travel greater distances and still return a strong signal. By conducting more current in a smaller footprint, GaN devices enable the design of compact lidar systems that can be easily integrated into the robot's structure without compromising performance.

Another key advantage of GaN in lidar systems is that its small size and chipscale packaging enable the minimization of parasitic inductances, which can degrade system performance. EPC has de-

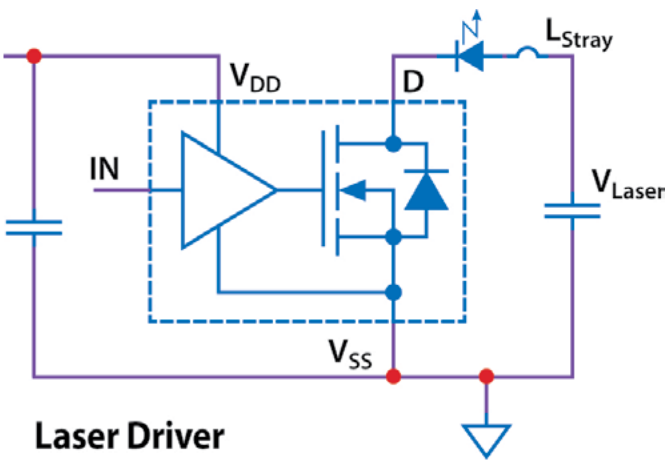

Figure 3: Typical connection using EPC21601 as a laser driver

veloped integrated circuits that combine a powerful GaN transistor with an integrated driver, effectively eliminating common source inductance and gate loop inductance. An example is the EPC21601, a 15 A, 40 V integrated GaN laser driver capable of over 100 MHz. Its 1 mm x 1.5 mm wafer-level package is compact, yet its solder bumps offer low inductance. Figure 3 shows the typical connection diagram for the EPC21601 as a laser driver. By integrating the transistor and driver into a single IC, EPC has improved the performance, reduced the size and cost, and increased the reliability of lidar systems in humanoid robots (The EPC9154 development board is available to help speed up new designs).

Powering the AI Brain: GaN in DC-DC Converters

The Need for High-Efficiency Power Supplies in AI Systems

The brain of a humanoid robot is its artificial intelligence (AI) system, which processes sensory data, makes decisions, and controls the robot's movements. AI systems are computationally intensive and require significant power to operate, especially when performing complex tasks such as real-time image processing, decision-making, and motion control. To meet these power demands, AI server power supplies rely on highly efficient DC-DC converters that can deliver power with minimal losses.

In humanoid robots, the AI system is responsible for processing data from sensors, making decisions, and controlling the robot's movements. This requires a constant supply of power, and any inefficiency in the power supply can lead to reduced performance, increased heat generation, and a shorter operating time. GaN-based DC-DC converters help to address these challenges by delivering power with minimal losses, ensuring that the AI system can operate at peak performance.

GaN in AI Server Power Supplies

The use of GaN in AI server power supplies provides a glimpse into the future of power electronics in humanoid robots. AI servers, which are produced by companies such as Nvidia, AMD, and Alibaba, require extremely high-power densities to fit within the limited space of a server board while delivering large amounts of power efficiently. GaN-based DC-DC converters have proven to be highly effective in meeting these requirements, offering power densities of over 5,000 watts per cubic inch with efficiencies approaching 98%.

One example of such a GaN-based DC-DC converter is the EPC9159 reference design, shown in figure 4, which measures just 23 by 18 mm and can deliver 1 kW of continuous power. This design achieves peak efficiency of more than 97.5% and full load efficiency over 95.5% when delivering 1 kW into a 12 V load. The compact size, combined with high efficiency, makes the GaN-based DC-DC converters an ideal solution for powering AI systems in humanoid robots, where space is limited, and power efficiency is critical.

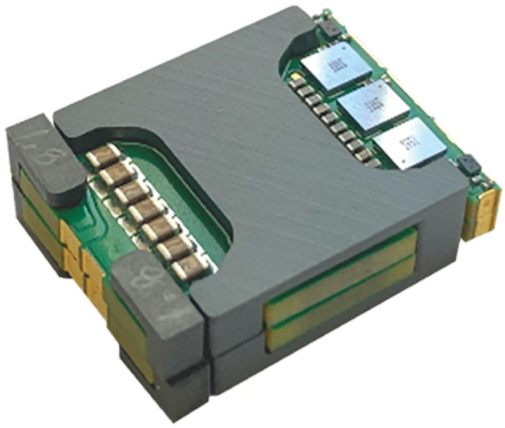

Figure 4: EPC9159 is a 1 kW, 48V/12V LLC Converter

GaN's Pivotal Role in the Future of Robotics

Humanoid robots are already being deployed in various environments. Semi-humanoid robots are delivering room service in hotels, serving as security guards in airports, and even delivering food on city streets. Soon, humanoid robots are expected to find high-volume applications in warehouses and factories, performing repetitive or dangerous tasks. As birth rates decline in developed countries, there is a growing concern about the availability of workers to support an aging population. Humanoid robots have the potential to fill this labor gap, helping to maintain economic stability and improve the quality of life globally.

As the global humanoid robot market continues to grow, the demand for advanced power electronics will only increase. GaN technology is uniquely positioned to meet this demand, offering superior performance, efficiency, and reliability compared to traditional silicon-based devices. Whether it's powering the motors that drive the robot's movements, the sensors that allow it to perceive and navigate its surroundings, or the AI systems that control its actions, GaN is the key to unlocking the full potential of humanoid robots. The ongoing advancements in GaN technology ensure the development of humanoid robots that are more efficient, reliable, and capable than ever before.

www.epc-co.com

2.5 kV IGBT Module in LV100 Package with Enhanced SLC+ Technology for Superior Power Cycling Performance

Mitsubishi Electric Introduces advanced 2.5 kV IGBT Module with Enhanced SLC+ Technology for Superior Power Cycling Performance. Engineered as optimal solution for 1000 Vac / 1500 Vdc 2-level inverters systems in wind, solar, hydrogen and energy storage applications. This new module sets a benchmark in reliability, tackling power and thermal cycling stress to ensure long-term stability and reduced maintenance costs."

By Thomas Radke, Akiyoshi Masuda, Mitsubishi Electric Europe B.V., Ratingen, Germany

Introduction

The global shift towards renewable energy sources like wind power, energy storage, hydrogen production, and photovoltaic (PV) systems is driving the need for power electronics that can deliver both high performance and exceptional reliability. Mitsubishi Electric is addressing these demands with a new generation of power modules that combine advanced packaging technology with cutting-edge chip design.

At the heart of this innovation is the Solid Cover+ (SLC+) structure, a significant update from the previous Solid Cover (SLC) technology [3]. The newly developed SLC+ structure is engineered to enhance power cycling capabilities, a critical factor in ensuring the long-term reliability of power modules under demanding operating conditions. This updated SLC+ structure is integrated with Mitsubishi Electric's latest low-loss 7th-generation 2.5 kV chipset, offering an ideal combination of performance and durability.

The 2.5 kV voltage rating has been specifically selected as the optimal solution for 1000 Vac and 1500 Vdc systems. This choice represents a carefully considered compromise between long-term DC stability (LTDS) and power losses, ensuring that the module provides both high efficiency and reliable performance in renewable energy applications. These new modules are tailored to meet the stringent requirements of high-performance applications in wind power, energy storage, hydrogen production, and PV systems.

With these innovations, Mitsubishi Electric is setting a new standard in power modules, focusing on maximizing both efficiency and reliability, even in the most challenging renewable energy environments.

Figure 1: LV100 module with 2.5 kV IGBT and SLC+ technology

Technical Innovation: The SLC+ Structure for higher reliability

Central to the enhanced performance and reliability of Mitsubishi Electric's new module is the Solid Cover+ (SLC+) structure. The well-known SLC structure [3] [2] has been update to for power cycling capability improvements.

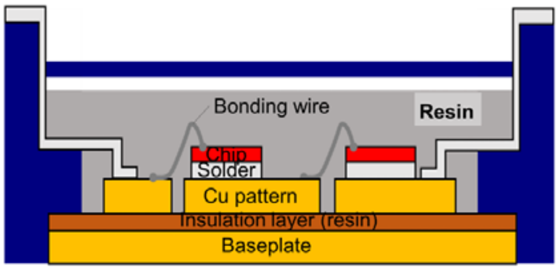

Structure name	Solid Cover (SLC)	Solid Cover + (SLC+)
module types	LV100	LV100
Sealing material	Resin	Resin
Substrate	Insulating metal substrate (IMS)	Insulating metal substrate (IMS)
Bond wire matrial	Al	Al-alloy
Chip surface	Metallization layer	Hard metallization layer

Figure 2: SLC and SLC+ technology

New Al-alloy Bond Wire:

The SLC+ structure introduces an advanced aluminum alloy bond wire that offers significantly higher yield strength compared to conventional bond wires. This enhancement is crucial as it directly addresses one of the primary causes of SLC module power cycle failure "bond wire cracking". Under power cycling, the repeated expansion and contraction of materials can lead to mechanical stress that eventually causes bond wires to crack. The new Al-alloy wire in the SLC+ structure is designed to withstand these stresses more effectively, increasing power cycling capability. This improvement not only extends the operational lifespan of the module but also enhances its reliability under the fluctuating temperature conditions typical e.g. in wind converter application. Especially the enhanced characteristics of the aluminum alloy wire in combination with the hard resin encapsulation of the SLC technology resulting in a significant improvement of power cycling capability.

AUTOMOTIVE HOME APPLIANCES INDUSTRIAL POWER TRANSMISSION RENEWABLES RAILWAY

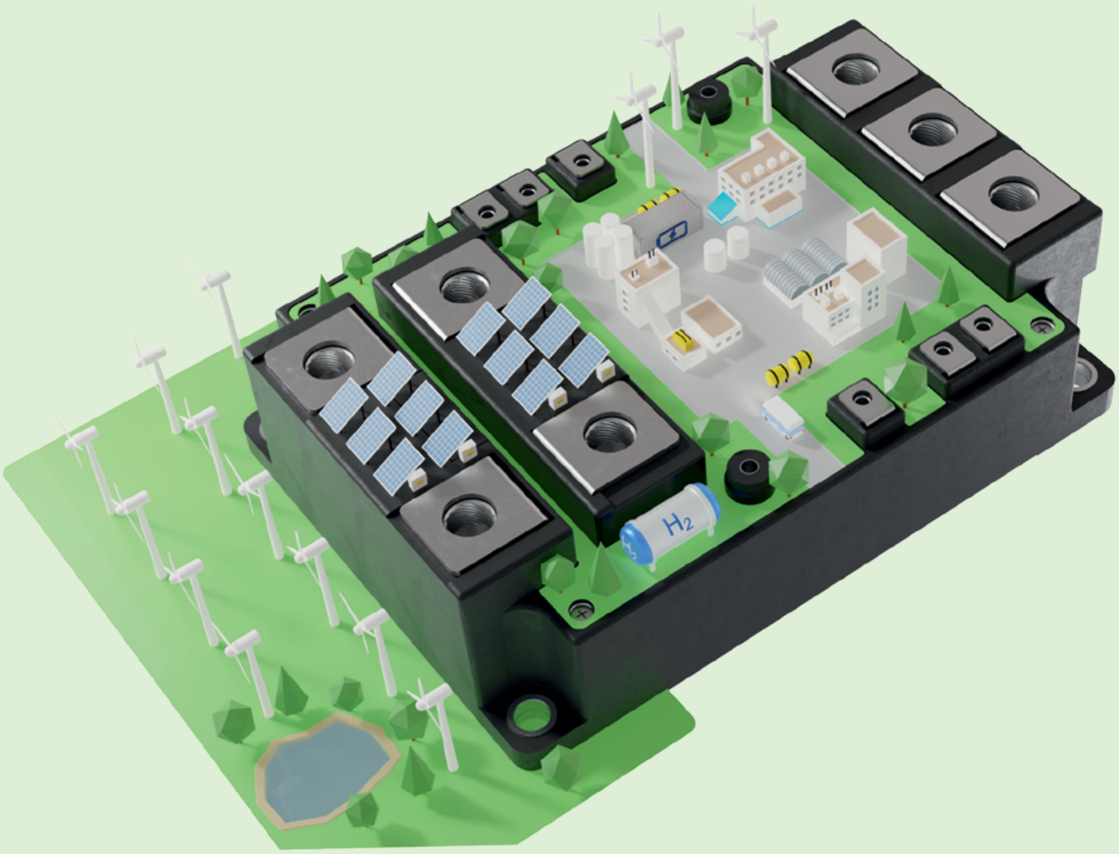

YOU CAN BUILD ON IT.

OUR POWER MODULES – YOUR GREEN DEAL.

Get all detailed information about the LV100 for Industrial and Renewables online at a glance

LV100: The standard package for future-proof industrial applications and renewable energies

- // Next generation high capacity standard package for industrial use
- // Scalability by easy paralleling
- // Enabling simplified inverter layout and assembly
- // High efficiency by latest 8th and 7th Gen. IGBT Technology
- // High current capability by 3 AC-output terminals
- // High thermal cycle capability by SLC-Technology
- // Pre-applied PC-TIM available
- // New 2000V class available enabling 2-level for 1500V_{dc} inverter systems
- // High temperature operation with $T_{vj\,max}$ = 175°C junction temperature at overload events
- // 2.5kV class and 1800A/1.2kV are under development

More Information:
semis.info@meg.mee.com
www.meu-semiconductor.eu

MITSUBISHI ELECTRIC
Changes for the Better

Hard Metallization Layer on Chip Surface:

Another critical feature of the SLC+ structure is the hard metallization layer applied to the chip surface. In traditional power modules, the chip electrode is susceptible to cracking due to mechanical stress and thermal expansion. Such cracks can lead to catastrophic module failures, rendering the entire system inoperative. The hard metallization layer in the SLC+ structure acts as a protective shield, preventing the formation of cracks and maintaining the integrity of the chip electrode. This innovation complements the improved bond wire, creating a synergistic effect that significantly enhances the overall robustness of the module.

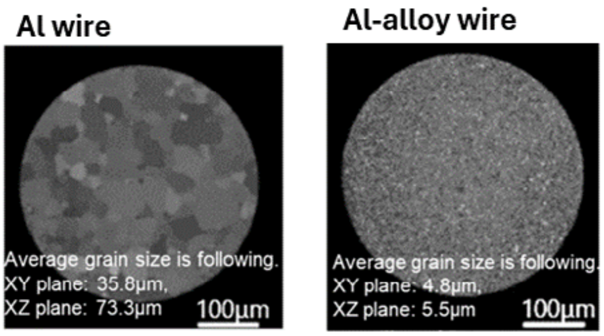

Wire material	Yield Str. (MPa)
Al	32
Al-alloy	87

Figure 3: Comparison of Al and Al-alloy wire

Power Cycle Performance Improvement

The actual benefits of the SLC+ structure are demonstrated through power cycling tests conducted by Mitsubishi Electric. These tests target is to reproduce the harsh operating conditions that power modules face in renewable energy systems, particularly the thermal cycling that occurs in wind turbine converters on generator side [1]. The 2.5 kV LV100 module with SLC+ structure exhibited a power cycling capability exceeding 40 million cycles under conditions of ton=0.1 s, Tjmax=150 °C, and ΔTj=50 K. Notably, this performance was achieved without any failures and demonstrate the effectiveness of the improved SLC+ structure design.

This represents a significant advancement over conventional power modules, which typically show signs of degradation or failure under similar conditions. The enhanced power cycling capability of the SLC+ module ensures that it can operate reliably over extended periods, even in the most demanding applications. This reliability is particularly critical in renewable energy systems, where unplanned maintenance or downtime can lead to substantial financial losses and disrupt energy production.

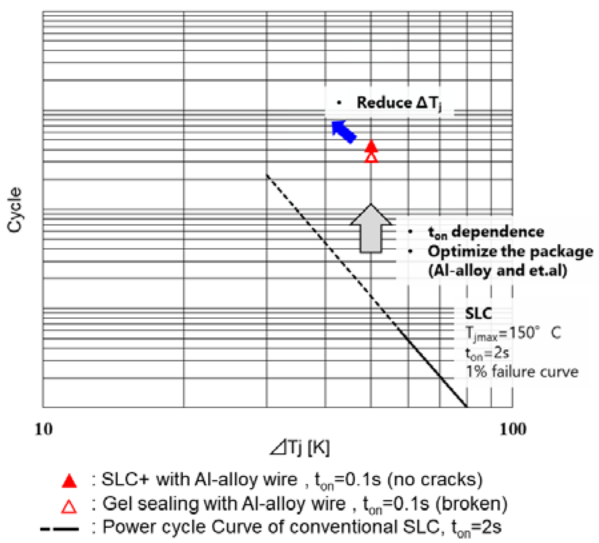

Figure 4: SLC+ power cycle test

2500V for low LTDS FIT rate

The 2.5 kV IGBT and diode chip-set used in this module have been optimized to meet the requirements of 1500 Vdc / 1000 Vac systems. This optimization involves achieving a delicate balance between minimizing power loss, controlling junction temperature, and enhancing long-term DC stability (LTDS) robustness. These factors are crucial in determining the module's efficiency and reliability. Also the chip sizes, the conduction and switching loss characteristics has been tuned to fit for converters in renewable application such as wind power and storage system. One of the key challenges in designing high-voltage modules is ensuring their robustness against cosmic rays, which can induce failures, especially in environments with long-term exposure to high DC voltages and or high altitudes. Cosmic ray-induced failures, though rare, can have catastrophic consequences, leading to sudden and unpredictable module failures. The 2.5 kV module's enhanced LTDS capability is the result of the 2.5kV chip design and , resulting in a outstanding lower FIT rate, making it an ideal choice for applications that demand long-term reliability and stability in combination with high efficiency.

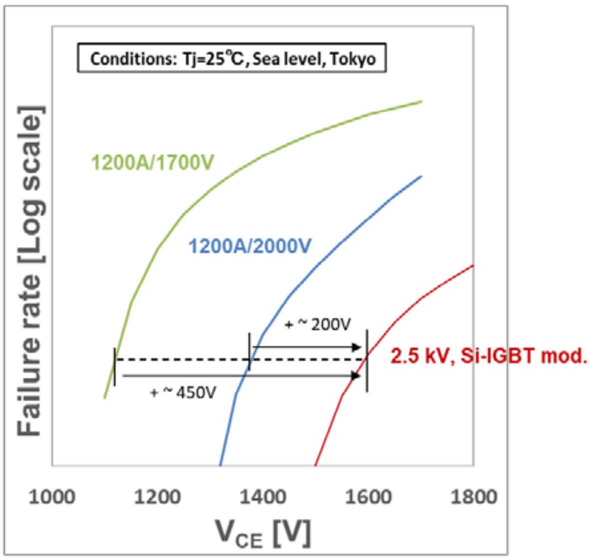

Figure 5: Estimation of LTDS failure rate

Module loss and thermal performance

The actual advantages of the 2.5 kV module with SLC+ structure are evaluated under typical application conditions from renewable applications. Simulations comparing the new 2.5 kV module with a standard 1.7 kV (CM1200DW-34T), module showing several key benefits particularly in wind power applications.

An excellent low loss switching performance has been achieved, as demonstrated in waveforms at 150 °C. Thanks to the LV100 package's reduced built-in stray inductance, the 2.5 kV module experiences low turn-off and recovery surges, resulting in smooth and rapid switching. This reduced inductance allowing a chip optimization towards loss reductions.

By keeping the same system output power while operating at higher voltage enabled by the 2.5kV module, the actual current can be reduced. The reduction of output current in the is enabling a slight increase in on state voltage without encroachment of overall performance. The 2.5 kV IGBT shows just about 15% higher on-state voltage compared to the 1.7 kV version, while the 2.5 kV diode only has a 5% higher forward voltage. The strong diode performance

IGBT:

Diode:

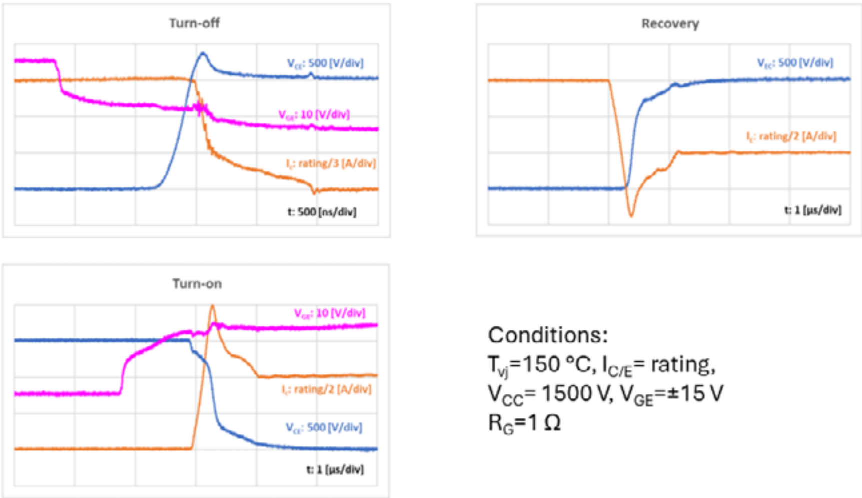

Conditions:
T_{vj}=150 °C, $I_{C/E}$= rating,
V_{CC}= 1500 V, V_{GE}=±15 V
R_G=1 Ω

Figure 6: Switching waveforms

has been designed because diode losses are critical in rectifier converters for wind s and hydrogen applications.

When comparing power losses and junction temperatures between the 2.5 kV and 1.7 kV modules, the 2.5 kV module delivers about 15% higher output power at the same junction temperature (150 °C). This is particularly beneficial in wind power systems, where the new module can achieve higher power output without exceeding thermal limits.

Moreover, thermally the 2.5 kV module has the improvement that the temperatures of IGBTs and diodes under typical operating conditions are very similar, which leading to efficient device usage and extended power cycling life-time since no device is causing a thermal or lifetime bottleneck while the other device is not fully. The reduced temperature swing (ΔTj) in the 2.5 kV module minimizes the diode as a bottleneck in negative power factor operating conditions and contributing to an extended power cycling lifetime

Conclusion

Mitsubishi Electric's new 2.5 kV IGBT module in LV100 housing, featuring the innovative SLC+ structure, represents a major leap forward in the design of power electronics for renewable energy applications. By addressing the key challenges of thermal and power cycling, power density, high efficiency and cosmic ray-induced failures, this module offers a reliable and efficient solution for renewable applications with 1500 Vdc or 1000 Vac inverter system.

The module's enhanced power cycling capability, coupled with high LTDS robustness and high efficiency features, makes it particularly well-suited for demanding renewable energy systems. As the industry continues to push towards higher efficiency and greater reliability, innovations like the SLC+ structure will play an important role in ensuring that power electronics can meet these demands. Mitsubishi Electric remains at the forefront of this technological evolution, committed to delivering advanced solutions that support the global transition to sustainable energy sources.

	1.7 kV module	2.5 kV module
Conditions		
V_{cc}	1000 V	1500 V
V_{out}	690 Vrms	1000 Vrms
$T_{vj(top)}$	150 ℃	
cosφ	-0.8	
f_c	1.5 kHz	
f_{out}	6 Hz	
Modulation method	3rd harmonic injection	
Modulation index	0.25	
Results		
P_{out}	1.1 MW	1.26 MW
$ΔT_j$ (IGBT)	32.3 K	45.8 K
$ΔT_j$ (diode)	53.7 K	44.2 K

Table 1: Thermal simulation results at wind converter operating conditions

Reference

[1] LI Hui et. al., "Power Cycling Capabilities Assessment of IGBT Modules in Wind Power Converter Considering the Wind Turbulence Effects" IEEE PEAC 2014.
[2] Takuya Takahashi et. al., "A 1700V-IGBT module and IPM with new insulated metal baseplate (IMB) featuring enhanced isolation properties and thermal conductivity", PCIM Europe 2016.
[3] Thomas Radke et. al., "More Power and Higher Reliability by 7th Gen. IGBT Module with New SLC-Technology", Bodo's Power Systems 2015.
[4] Tsuyoshi Uraji et. al., "Increase of Power Cycling Lifetime in Power Semiconductor Modules Applied Fine-Grained Al Alloy Wire" Mate 2022.

www.mitsubishielectric.com

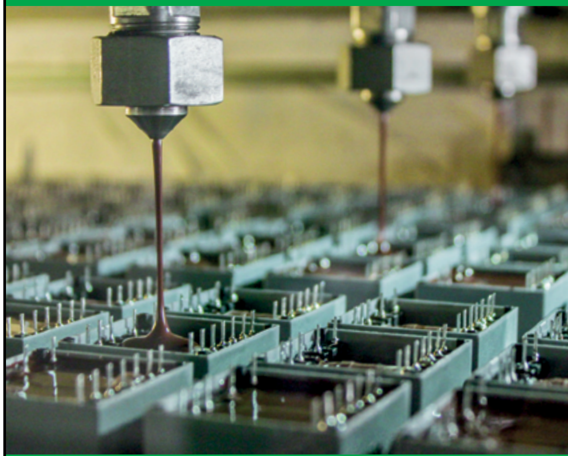

Meeting Grid Code Requirements for High Power Electrolyzers; Choosing the Right Power Electronics Topology

In the rapidly evolving world of power electronics, where cutting-edge technologies like IGBT, GaN, and SiC MOSFETs dominate, advocating for the decades-old thyristor might seem counterintuitive. However, for high-power hydrogen production via electrolysis, the humble thyristor proves to be exceptionally effective and efficient.
This might surprise those who view thyristors as outdated, but the unique demands of large-scale electrolysis reveal that thyristors aren't just viable—they're the best option.

By Mohamad El Ghouti – Technical Marketing Manager at Infineon Technologies Bipolar

Introduction: Thyristors in Electrolysis – A Contrarian Perspective
In the rapidly evolving world of power electronics, where cutting-edge technologies like IGBT, GaN, and SiC MOSFETs dominate, advocating for the decades-old thyristor might seem counterintuitive. However, for high-power hydrogen production via electrolysis, the humble thyristor proves to be exceptionally effective and efficient. This might surprise those who view thyristors as outdated, but the unique demands of large-scale electrolysis reveal that thyristors aren't just viable—they're the best option.

Imagine this: You're tasked with designing a power electronics system for a high power electrolyzer (>10 MW) that must convert vast amounts of electrical energy into hydrogen by connecting an electrolyzer plant into the grid. You need a solution that is not only robust and reliable but also cost-effective, compact, and highly efficient.

Consider the Thyristor, a semiconductor device that excels in precisely these areas. Its cost effectiveness and ability to conduct high currents with minimal losses, combined with its proven reliability over decades of use, makes it the ideal choice for hydrogen production.

Yet, a common pitfall experienced and fresh engineers fall into is misinterpreting the significance of grid codes. There's a misconception that thyristor-based topologies cannot meet grid code requirements, leading to their dismissal. As a result, engineers opt for more expensive and less reliable systems that are not optimized for high-power electrolysis.

This paper debunks the myth that thyristors can't meet electrolyzer demand due to strict grid codes. By looking into specific requirements of the VDE-AR-N 4110, the German grid code for medium voltage network connections, we will reveal why thyristors are actually the best choice for high-power electrolysis. Through a comprehensive analysis, we will highlight instances where thyristors emerge as the superior choice for high-power electrolysis, marrying efficiency and compactness with reliability and cost-effectiveness.

Type of installations and Grid Code Classifications
To successfully integrate high-power electrolyzers into the grid, it is essential to understand the grid code requirements at the Point of Common Coupling (PCC). According to "VDE-AR-N 4110," there are three PCC installation types (see Figure 1).

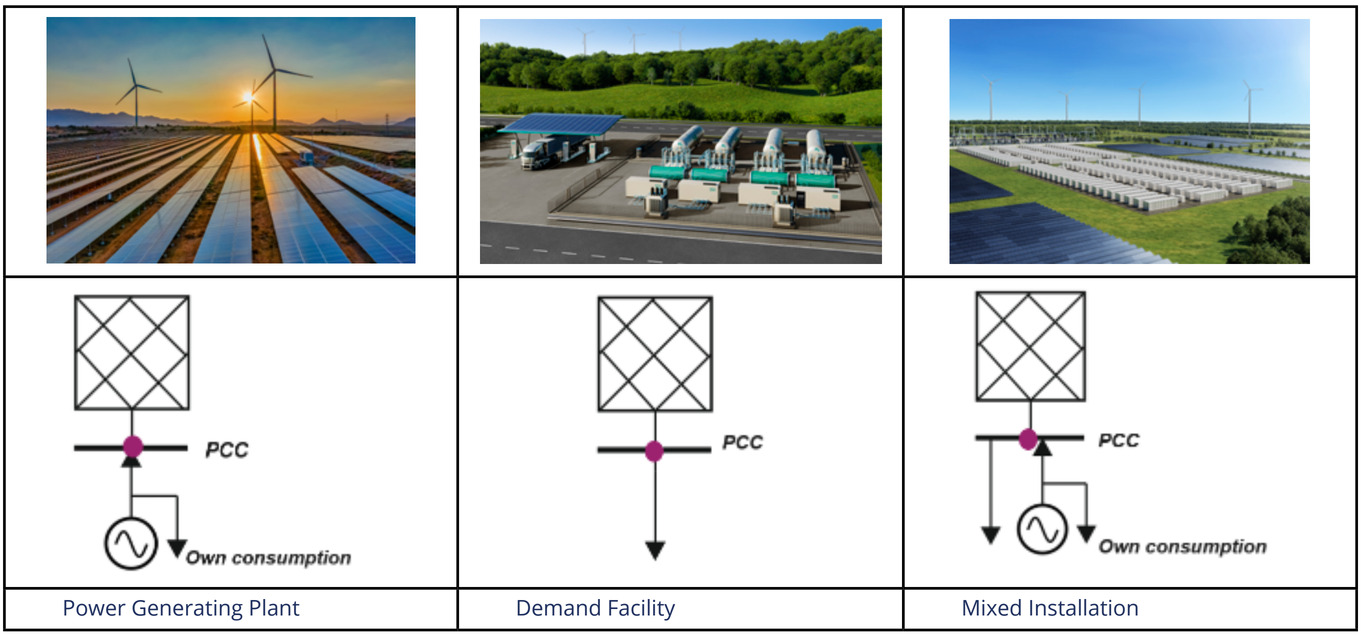

Figure 1: Installations according to VDE-AR-N- 4110

PCC installation types per VDE-AR-N 4110:

- **Power generating plant:** installation with power generating units and necessary electrical equipment required to operate the installation.
- **Demand Facility:** customer installation that solely consumes electrical energy from the network.
- **Mixed Installation:** a combination of demand facility and power generating plant.

An electrolyzer is classified as a demand facility or a mixed installation if it includes a power generation source or battery at the PCC. Demand facilities must manage harmonics and maintain a high power factor (>0.95), while mixed installations face stricter requirements like reactive power control, frequency control, fault ride-through capabilities, etc...

Most high-power electrolyzers are demand facilities, mainly required to meet harmonic and power factor standards. Additionally, the installation location significantly influences the requirements at the connection point. Typically, electrolyzers connect to either:

- **Public Grid:** Electrolyzer plants connected to the public grid must adhere to all grid operator regulations. For a demand facilities, this mainly involves meeting harmonics and power factor requirements.
- **Industrial Grid:** Connected to an industrial or chemical park's private network. Here, the grid owner typically meets the grid operator's requirements at the PCC, usually at high voltage (HV). Within this private network, the electrolyzer generally has no specific obligations unless explicitly requested by the network operator.

Besides the installation's location (public or industrial grid), the grid strength at the PCC significantly influences the choice of power electronic topology. Grid strength can be categorized into two types:

- **Robust Grid:** SCR [1] > 10, grid can handle more significant disturbances and have higher fault levels.
- **Weak Grid:** SCR < 10, grid is more susceptible to disturbances, requiring careful management of power quality and stability.

The choice of the electrolyzer power supply system and power electronic topology should be determined by the type of installation, grid location (public or industrial), and grid strength

Dominant Power Electronics Topologies for Electrolyzer Demand Facilities:

Choosing the appropriate power electronics topology for electrolyzers is crucial for efficient operation and compliance with grid requirements. Figure 2 illustrates the most prevalent power electronic topologies.

1. **12P-Thyristor (B12C Configuration):** uses a 12-pulse transformer and a tap changer with two rectifiers connected in parallel. It is highly reliable, compact, and efficient for demand facilities on robust industrial grid.
2. **12P-Thyristor + Compensation:** Add active or passive compensators to the 12P-Thyristor to manage harmonics and improve power factor. It is particularly effective for public robust & weak grids needing better power quality.
3. **Active Front-End (AFE):** A 2-level IGBT-based converter offering advanced control over harmonics and power factor, suitable for public weak grid but comes with higher capital and operational costs.
4. **Diode-Based Rectifier with IGBT Chopper:** Combines a diode rectifier and an IGBT chopper for DC control. This topology is suitable for both public and industrial weak and robust grids. This topology suits both public and industrial grids, whether weak or robust. Although flexible, it is generally less efficient than thyristor-based solutions, and becomes less favorable for electrolyzer plants exceeding 20 MW.
5. **AFE with Chopper:** Merges AFE with IGBT chopper for top-tier control and performance. Optimal for very weak public grids; however, it is significantly more expensive.

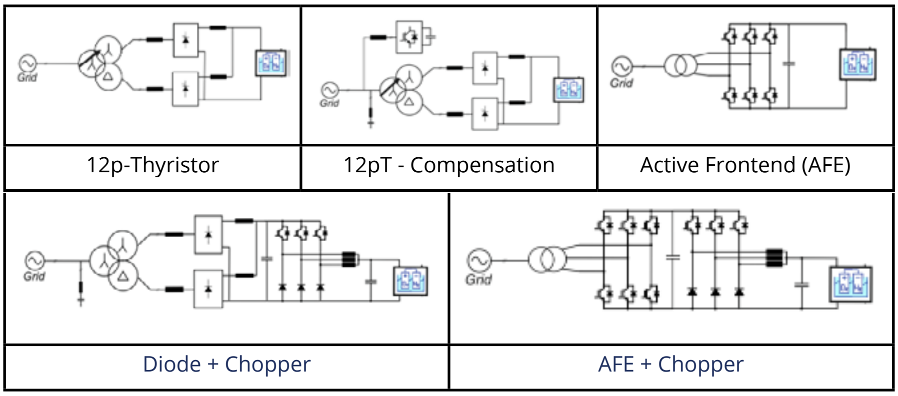

Figure 2: Relevant power electronics topologies for electrolyzers

Criteria	**12P-Thyristor**	**12P-Thyristor + Compensation**	**AFE**	**Diode + Chopper**	**AFE + Chopper**
Grid location	Industrial	Public & Industrial	Public	Public & Industrial	Public
Grid strength	Robust	Robust & weak	Robust & weak	Robust & weak	weak
Reliability	++++	+++	+	++	0
Compactness	++++	+++	+	++	0
Efficiency	99.5%	98.6%	98.08%	98.08%	96.6%
Power Factor	0.92 **	0.98 **	0.99	0.98	0.99
THD [%]	9	< 5	1.5	< 5	1.5
CAPEX/OPEX [2]	lowest	Low	High	Moderate	highest

Table 1: Topology selection guide

Selection Guide: Optimal Topologies for Different Scenarios

To help in selecting the best topology for your application, consider the following comparison of key factors across different topologies:

Case Study: The Economic Impact of Efficiency

In high-power systems like a 10 MW electrolyzer, even a small increase in efficiency can lead to substantial savings. For instance, consider the difference between a 12P-Thyristor + Compensation system with 98.6% efficiency and an Active Front-End (AFE) system with 98.08% efficiency. Although the efficiency gap is just 0.53%, the impact is significant. Over a year, the 12P-Thyristor + Compensation system consumes+ 380.4 MWh less energy than the AFE system. With electricity costing 10 cents per kWh, this results in an annual cost saving of approximately $38,040. Now, if you scale this to a 100 MW electrolyzer system, the yearly savings would increase to about $380,400, highlighting how thyristor-based rectifiers not only improve efficiency but also significantly reduce operational costs, making them a more economical choice for hydrogen production.

Infineon Bipolar Technologies: Offering a Range of Thyristor Solutions

Infineon Technologies Bipolar provides a comprehensive range of high-performance thyristors and stacks for high-power applications, including hydrogen production via electrolysis (see Figure 3). Our thyristors offer exceptional efficiency and reliability, while our stacks simplify rectifier development, speeding up time to market and reducing design complexity. These solutions cover a wide voltage range and offer both forced air and water cooling options, catering to diverse client needs and maximizing system performance.

Conclusion

Thyristor-based power electronics topologies provide an optimal solution for high-power electrolyzers, particularly when connected to industrial or public grids. Their ability to deliver high efficiency, reliability, and cost-effectiveness makes them the top choice for industries focused on hydrogen production. As the demand for green hydrogen grows, embracing thyristor technology will be key to achieving both technical and economic success in this emerging energy sector.

Water cooled B6C stack (Module Thyristor)

Air cooled B6C stack (Disc Thyristor)

Water cooled B6C stack (Disc Thyristor)

References

[1] SCR is defined as the ratio of the short circuit power (or short circuit capacity) at the PCC to the rated power of the connected load, such as a power electronics system

[2] The analysis considers the whole power supply system from the PCC till the electrolyzer. That includes transformer, tap changers, active and passive compensators, and the rectifier.

www.ifbip.com

ANPC Converter Design for Efficient Energy Storage Systems

Without sufficient storage, switching to renewable energy will not be sustainable. Therefore, Battery Energy Storage Systems (BESS) are a true growth opportunity. A doubling of new energy storage installations globally from 2022 to 2023 has driven a change in the approach to power converter design for utility-scale systems. With an appropriate design semiconductor efficiencies above 99 % can be achieved.

By Paul Drexhage, Senior Technical Marketing Manager, Semikron Danfoss

The on-going shift to renewable energy sources requires energy storage to ensure a continuous and reliable supply of energy at the grid. Massive growth in BESS installations has been driven by government mandated renewables projects where energy storage systems must be co-located with generation. Additionally, advances in battery technology have increased the power density of BESS containers, making installations feasible in areas with limited footprints.

The potential for BESS to provide grid stability is yet to be fully exploited. They can provide peak shaving, load shifting, and backup power through integration into applications such as data centers. These applications have so much growth potential that the International Energy Agency predicts a growth in the cumulative global installations of utility-scale batteries from 54 GW in 2023 to more than 500 GW in 2030.

BESS Design

Utility-scale, AC-coupled BESS have traditionally relied on the same central inverter approach as solar, where a single inverter was fed from a bank of batteries (Figure 1). The power conversion system (PCS) consisted of a MW-scale, bi-directional 2-level (1000 V) or 3-level (1500 V) voltage source inverter. This system, packaged in a 20-foot container, was seen as cost-effective as it used existing inverter designs from already developed (and co-deployed) solar equipment. However, experience has shown that this configuration can cause serviceability challenges as a single failure in the inverter would render the entire system unusable. Furthermore, the increasing diversity of BESS installation locations means that more granularity is required for battery bank sizes.

Figure 1: BESS container with central inverter.

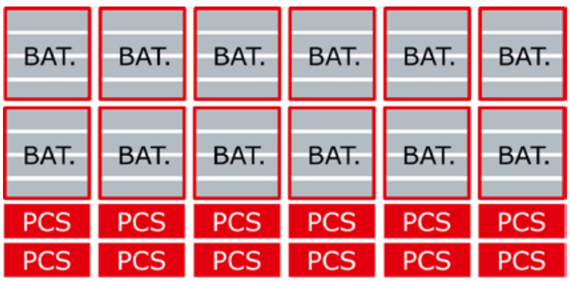

Figure 2: BESS container with modular PCS.

The modular PCS approach (Figure 2) is the current trend to resolve these issues. The same 20-foot container is used but each rack of batteries has its own dedicated inverter. This improves serviceability, as only one subset of batteries is taken offline when a PCS failure occurs. Furthermore, it is now possible to change system power rating in increments of one battery rack without worrying about the inverter being oversized for the application.

Advancements in battery technology are also influencing PCS sizing. Lithium-ion (Li-ion) remains the predominant battery type. However, there have been consistent developments in material optimization, electrolyte innovations, and manufacturing technology. New Li-ion types such as cobalt-free Lithium Iron Phosphate (LFP) allow 5 MWh of capacity in a 20-foot container. Recent improvements will push this power rating to 6 MWh and beyond in the next few years.

While the "energy capacity" of the BESS is one value (e.g. 6 MWh), the "rated power capacity" of the system for charging/discharging is lower. This is the power level at which the entire system could be instantaneously discharged starting from a full charge. A fractional value, designated with a P or C, defines this rate and, hence, the power rating of the PCS.

At a 0.5C charge/discharge rate, this means that the PCS in a 6 MWh BESS needs to be rated for 3 MW continuous operation. With the 12-rack topology shown in Figure 2, a power rating of approximately 250 kW per PCS is needed. Couple this with the fact that a modern rack-mounted PCS must fit into a standard 19" wide rack and it is clear that power density becomes a driving factor when designing a power converter. Additionally, critical requirements for the PCS are as follows:

- Ability to accept up to 1500 VDC continuously
- High efficiency over charging (PF = -1) and discharging (PF = 1) modes
- Power dense (liquid cooling)
- Withstand repeated system (long) charge/discharge cycles

PCS Design

Today, the most effective topology for meeting the electrical requirements is the 3-level, active neutral point clamped (ANPC) converter. The 3-level configuration can accommodate the 1500 V bus voltage using low loss 1200 V semiconductors. The ANPC configuration (as opposed to the NPC type) offers equally high efficiency when the battery is charging (PF = -1) and discharging (PF = 1).

The SEMITOP E2 power module from Semikron Danfoss packages all six switches in an ANPC phase leg into a compact footprint (57 mm x 63 mm). Press-fit or solder pins allow for easy PCB mounting. The one-piece housing with integrated mounting tabs applies high mounting pressure to the heatsink. This mechanical design feature alone provides a superior thermal resistance, $R_{th(j-s)}$, to industry standard modules. However, the SEMITOP E2 is also available with pre-applied high performance thermal paste (HPTP) or

phase change material (HP-PCM) in an optimized pattern for best-in-class thermal performance. A baseplate-less design strongly benefits from a liquid cooled heatsink and minimizes the thermal layers between the chips and coolant. The lack of baseplate and the associated solder layer means that the module is resilient against thermal cycles that come with each charge and discharge event.

Since control methodology of the ANPC converter strongly affects individual switch losses, the power module must be designed with chips optimized for either conduction or switching losses in each switch position. The 150A ANPC SEMITOP E2 (Figure 3) is designed for the Low Frequency/High Frequency (LF/HF) switching scheme. This means that the four switches in positions T1, T5, T6, and T4 are Generation 7 high power IGBTs. These IGBTs are designed for low conduction losses as they only switch with the line frequency. The two switches in positions T2 and T3 are the latest generation silicon carbide MOSFETs. The switches in these positions operate at a high carrier frequency and must exhibit low switching losses. This hybrid approach allows for high frequency switching for LF/HF configurations while keeping the overall module cost low.

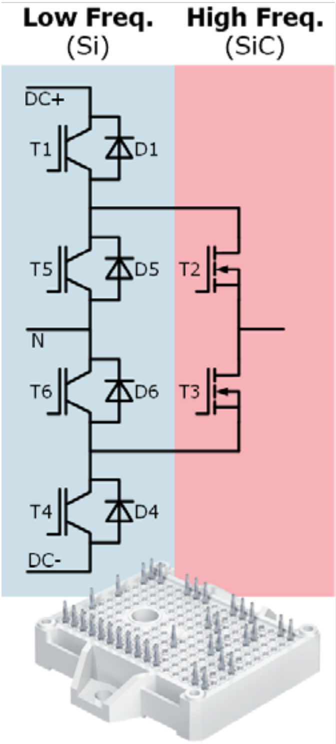

Figure 3: SEMITOP E2 module (e.g. SK150AMLI120CR03TE2)

The specification for a future-looking, modular PCS used in multi-MW class containers is given in Table 1. This has been used as the basis for a thermal simulation of a PCS design using the SEMITOP E2 module.

To meet the target power output and charge/discharge lifetime while still maintaining adequate efficiency, two SK150AMLI120CR03TE2 are used in parallel to construct each of the three phase legs. These have been placed on a hypothetical water-cooled heatsink (Figure 4) with a total $R_{th(s-a)}$ of 0.0146 K/W. All six modules fit within a 400 mm x 58 mm footprint.

The results (Figure 5) show that semiconductor efficiencies above 99 % can be achieved across a switching frequency range of 10...20 kHz while either charging or discharging.

Parameter	Value
V_{DC} [V]	1500
V_{AC} [V]	690
I_{AC} [A]	209
Grid frequency [Hz]	50
Power [kW]	250
Cooling	Liquid, $T_{coolant}$ = 50 °C

Table 1: Next generation modular PCS specification.

A Modular PCS for Everyone

Design of a complete PCS requires a knowledge of 3-level power converter control, as well as system and application knowledge to ensure that the PCS interacts properly with the whole BESS. This is where a power electronics developer experienced with renewable energy resources is helpful. Semikron Danfoss is partnering with Headspring Inc. of Tokyo, Japan to develop an exemplary PCS around the SEMITOP E2 module.

Headspring is developing the ANPC control software to drive the power modules using their high-speed real-time controller system. This controller will also integrate connections with the BESS battery management system (BMS), as well as functions for a code-compliant grid-tied connection. An option for standalone mode is available as well, which allows the BESS to function as a reliable backup power source during grid outages.

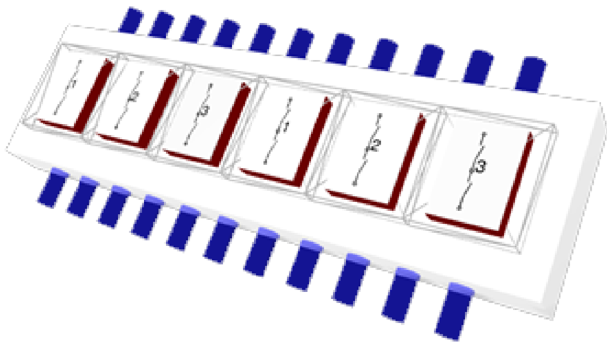

Figure 4: Simulated hypothetical water-cooled heatsink configuration for six SEMITOP E2 modules (2 per phase).

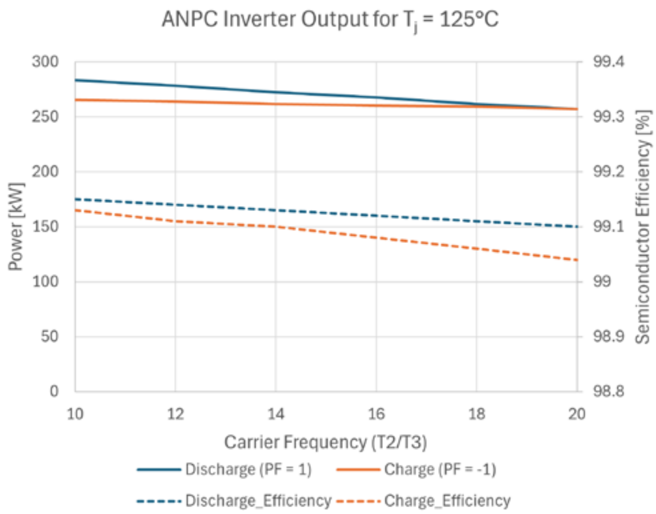

Figure 5: Output power and efficiency of ANPC inverter (semiconductor losses only).

Each PCS module has its own controller designed to seamlessly integrate with other PCS modules connected in parallel. This provides the scalability needed to drive the entire BESS container as well as providing continued system operation in case of failures of individual PCS modules. Headspring is also experienced with designing filters and protection circuits necessary for the PCS.

For the power converter hardware, Semikron Danfoss can provide design support to integrate SEMITOP E2 power modules with Headspring control systems. With this collaboration, anyone building utility scale BESS can get access to a next-generation modular PCS design.

Summary

Advances in application requirements and battery technology are changing the way high power BESS are designed. A modular PCS block based on the ANPC topology is presently the optimal solution. With power electronics from Semikron Danfoss and controls from Headspring, an advanced solution is available to everyone.

www.semikron-danfoss.com

Worried that your subscription could end abruptly?

Your tool.

PLECS.

A perpetual PLECS license means you can choose to pay for upgrades, but the tool is yours forever

plexim

electrical engineering software

Towards Vertical GaN Power ICs

Two trends are currently emerging in GaN power technologies: One the one hand, the monolithic integration of system peripherals to the power transistor, which can reduce system costs, the bill of materials and, last but not least, improve performance. On the other hand, vertical transistors are being developed to increase breakdown voltages and thus achieving higher switching power. Combining lateral and vertical geometry is the aim of Fraunhofer IAF with the development of vertical GaN power ICs and their related technologies.

By Michael Basler, Richard Reiner, Stefan Mönch, and Philipp Döring, Fraunhofer Institute for Applied Solid State Physics (Fraunhofer IAF)

Combining the best of both worlds is the motto behind the development of vertical GaN power ICs. The lateral GaN technology with its HEMT-design has revolutionized the field of power electronics as it offers significant performance advantages and increasingly lower costs compared to conventional Si-based power transistors. Another benefit of the lateral structure is the potential of integrating active or passive devices to the GaN power HEMT on-chip, enabling functions like gate drivers, sensing or protection circuits—known as a GaN power IC or GaN power integration. However, commercial lateral GaN transistors currently have a limited breakdown voltage of typically 650 V (in some cases even 1200 V since a few years) and a switching power capability of a few kilowatts. The aim is to overcome these limitations with vertical GaN transistors, which also have the advantage of increasing the breakdown voltage without enlarging the chip size. Furthermore, the reliability and thermal management can be improved by moving the peak electric field and dissipation of heat from the surface into the bulk substrate. There are four major vertical GaN device approaches such as Trench MOSFET, FinFET, JFET, and CAVET (current aperture vertical electron transistor). Toyoda, Panasonic, or Start-Ups like Oddysey Semiconductor and the recently dissolved NexGen Power Systems already showed promising normally-off vertical GaN transistors, but these are not yet commercially available. One of the biggest challenges currently facing vertical GaN devices is their economic viability, mainly due to the high cost of GaN wafers. Today, 6-inch GaN substrates are under development, while 2- and 4-inch are in mass production [1], but the cost of wafer including epitaxial layers is currently high at 40-60\$/cm² compared of ~7\$/cm² for 4-inch SiC [2] or ~1\$/cm² for 8-inch GaN-on-Si [2]. This relatively high price must be reduced to ensure the breakthrough of vertical GaN transistors despite a theoretical improvement in the unipolar $R_{ON}\times A$ figure-of-merit compared to SiC MOSFETs. In the above-mentioned vertical device structures, only the CAVET features the same heterostructure as the conventional HEMT with the same gate module. While different epitaxial layers are used as vertical depletion zone, the process technology can be widely adopted from the known lateral devices. This unique selling point of the CAVET opens a way to continue lateral GaN power integration in vertical device concepts to a vertical GaN power IC (see Figure 1) and could become a promising vertical structure of the future.

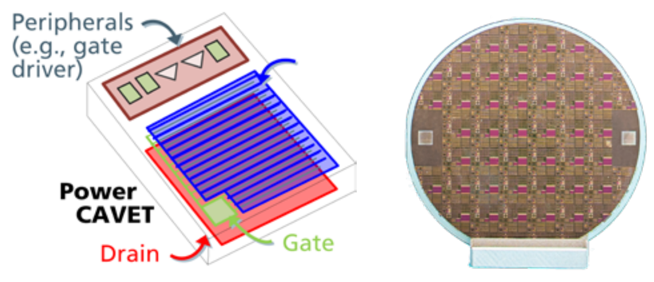

Figure 1: a) Schematic 3D view of a vertical GaN power IC and b) photograph of a fully processed 2-inch GaN-on-GaN wafer.

Co-Integration of Lateral HEMTs and Vertical Power CAVET

The Fraunhofer IAF has developed a technology, which combines a co-integrated large-area vertical GaN power transistor with lateral devices for the realization of peripheral functions on a single chip. The aforementioned CAVET combines a well-known gate module of the lateral HEMT with a vertical depletion- and drift-zone. Consequently, the same normally-off concepts used for the HEMT (e.g., p-GaN gate) can be applied to the CAVET. This technology starts with a highly negatively doped (n^+) GaN substrate and subsequent homoepitaxy, which has significantly better dislocation densities than heteroepitaxy on foreign substrates such as Si or Sapphire and can therefore positively influence breakdown voltage and reliability. With the help of MOCVD (metal-organic chemical vapor deposition), a weaker n-doped (n^-) GaN layer with a few micrometers is grown on top, which serves as a depletion- and drift-zone. A positively doped (p) GaN current blocking layer (CBL) is then manufactured by Mg-implantation, which acts as an insulating layer separating the source from the drain, while an aperture allows vertical current flow below the gate area. Finally, an un-intentionally doped (uid)-GaN channel, an AlGaN heterostructure and a GaN cap or alternatively p-GaN are regrown above, which build the access region of the vertical transistor and the channel region of the lateral HEMTs. The devices are fabricated in our III-V process line. Details on the epitaxy and fabrication can be found in [3–6]. The same active and passive components as in the lateral GaN technologies are available. Figure 1b) shows fully processed 2-inch GaN-on-GaN wafer, which could also be realized on larger diameters in future. A simplified cross-section of the technology and a TEM cross-sectional image of a fabricated CAVET are shown in Figure 2a) and c).

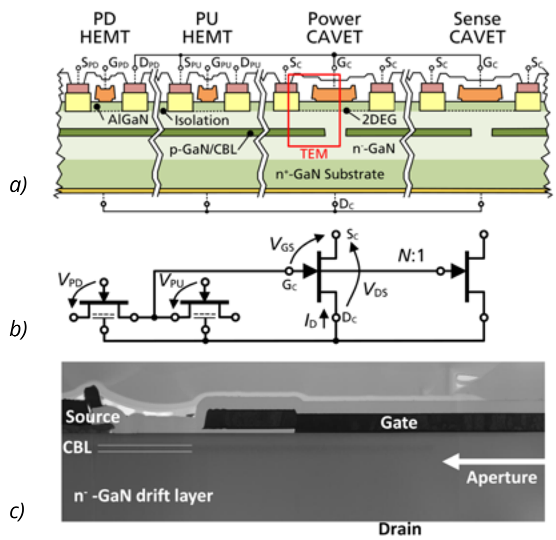

Figure 2: CAVET technology with quasi-monolithic integrated HEMT gate driver stage and sense CAVET as a) simplified cross-section and b) corresponding circuit diagram. c) TEM image of a section of the vertical CAVET device marked in red in a).

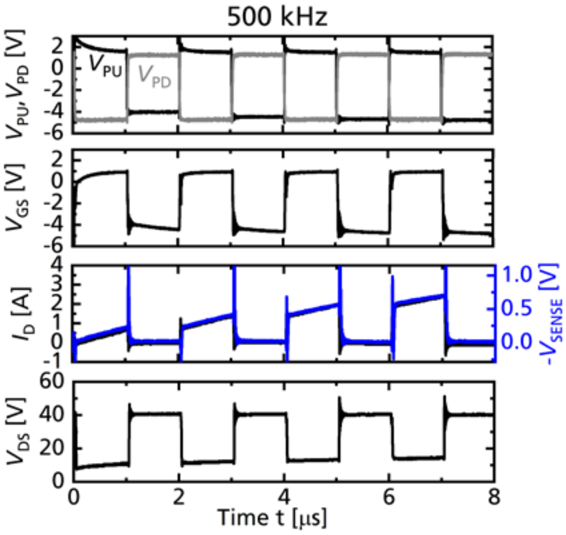

Figure 3: Switching measurement of the power CAVET device controlled by lateral co-integrated HEMTs and sense CAVET at 500 kHz and 40 V.

Experimental Results

To demonstrate the development towards vertical GaN power ICs, several vertical and lateral devices were manufactured in the same technology. After processing, the components were diced for flexibility reasons, but should behave like monolithically integrated on one die/chip if the backside or drain potential D_C is the same or connected together, see circuit diagram in Figure 2b). The experimental proof-of-concept is shown using a large-area CAVET power device controlled by a quasi-monolithically integrated lateral HEMT push-pull driver stage with current sensing via a sense CAVET. Figure 2b) shows the corresponding circuit diagram/symbols and indicates the current direction (lateral vs. vertical) by the orientation of the symbols. The push-pull HEMT stage consists of a pull-up/down (PU/PD) transistor and the current-mirror ratio N is ~229.

The GaN-based devices were statically characterized in detail and presented in [3–6]. The dynamic switching measurements are carried out in a double-pulse test setup at 40 V, up to 2.4 A, and 500 kHz and the gate-source voltage of the PU/PD device V_{PU}/V_{PD}, the gate-source voltage of the power CAVET V_{GS}, which corresponds to the V_{GS} of the sense CAVET, the drain-current I_D and drain-source voltage V_{DS} of the power CAVET are shown in Figure 3. The drain current of the power CAVET is measured by a voltage drop of a coaxial shunt and the mirrored current through the sense transistor is converted into the voltage V_{SENSE} using an external transimpedance amplifier. Further details of the GaN gate driver stage with more switching measurements are given in [4] while more information on the current monitoring is given in [5].

Summary

The development of vertical GaN power ICs aims to merge the benefits of lateral GaN technology with a vertical transistor structure. Not only traditional parameters such as higher voltage and current should be addressed, but also the advantage of monolithic functional integration and the associated reduction in system costs. This is intended to provide a further sales argument for the vertical GaN transistors, which are currently still in an early development state, and commercially rarely available. However, the research results show their great potential. Vertical GaN power ICs will push the performance of this technology even further and will be continued in ongoing projects at Fraunhofer IAF.

References

[1] SUMITOMO CHEMICAL, Sumitomo Chemical to Attend APEC 2024 Exposition to Exhibit its CompoundSemiconductor Products for Next-Generation Power Devices | Announcements | SUMITOMO CHEMICAL. [Online]. Available: https://www.sumitomo-chem.co.jp/english/news/detail/20240207e.html (accessed: Jul. 18 2024).
[2] Y. Zhang, A. Dadgar, and T. Palacios, "Gallium nitride vertical power devices on foreign substrates: a review and outlook," Journal of Physics D: Applied Physics, vol. 51, no. 27, p. 273001, 2018, doi: 10.1088/1361-6463/aac8aa.
[3] P. Döring et al., "Technology of GaN-Based Large Area CAVETs With Co-Integrated HEMTs," IEEE Transactions on Electron Devices, pp. 1–6, 2021, doi: 10.1109/TED.2021.3109840.
[4] M. Basler, P. Döring, S. Mönch, R. Reiner, M. Mikulla, and R. Quay, "Switching of GaN CAVET With Quasi-Monolithic Integrated HEMT Gate Driver," IEEE Electron Device Letters, vol. 44, no. 8, pp. 1332–1335, 2023, doi: 10.1109/LED.2023.3290608.
[5] M. Basler et al., "Vertical GaN Transistor with Quasi-Monolithically Integrated HEMT Gate Driver and Sense-CAVET for Current Monitoring," in 2024 IEEE Applied Power Electronics Conference and Exposition (APEC), Long Beach, CA, USA, 2024, pp. 737–741. [Online]. Available: https://ieeexplore.ieee.org/stamp/stamp.jsp?tp=&arnumber=10509173
[6] P. Döring et al., "Towards Vertical GaN-Power ICs: Co-integration of Lateral HEMTs and Vertical Power CAVETs," in 2024 36th International Symposium on Power Semiconductor Devices and ICs (ISPSD), Bremen, Germany, 2024, pp. 382–385. [Online]. Available: https://ieeexplore.ieee.org/stamp/stamp.jsp?tp=&arnumber=10579561

www.iaf.fraunhofer.de

Cutting-Edge Transfer Molded Module for High-Performance Vehicles

The traction inverter is the heart of the e-mobility revolution. It is responsible for electrical propulsion as well as the vehicle's performance in terms of mileage. Carmakers demand extremely high performance from both electrical and thermal aspects, compelling semiconductor companies to improve technology. This includes transitioning from standard silicon to silicon carbide and introducing new materials and cooling systems.

By Domenico Nardo, Power Specialist for Automotive Applications, and Roberto Maugeri, Senior Applications Engineer, both STMicroelectronics

Traction inverter trends and new requirements

The key elements of electrical traction are the e-motor and the traction inverter. Both components are significantly impacted by requirements for efficiency, compactness, car mileage, and thermal management.

To increase the peak power of BEVs and improve efficiency, there is a shift from 400V battery voltage to 800V. Higher battery voltage reduces charging time and copper losses in the wires, which also helps reduce conduction losses in the inverter's power stage.

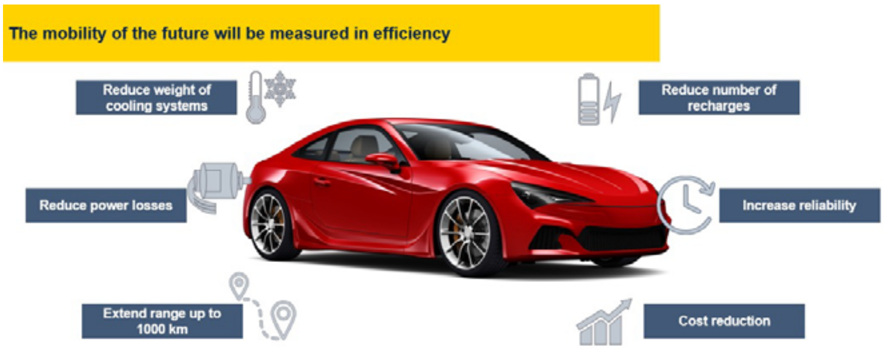

Figure 1: Main requirements for the new BEV

Current level for different bus voltage for 400kW peak power		
$V_{battery}$ (V)	400	800
I_{DC} (A)	1000	500

Table 1: Current and bus voltage for a 400kW inverter

Conduction losses are predominant in such applications and have a quadratic relationship with the current. Alongside increasing bus voltage, significant research and development are focused on improving the dimensions of the traction inverter to make it lighter and more compact. This is achieved through new power module attachments to the heatsink, such as silver sintering, new materials, and new package concepts.

Moving from 400 V to 800 V battery systems

New motor architectures

- Axial flux
- Synchronous reluctance
- External flux motor
- increasing motor speed

Improving EV powertrain

- Optimize power density, efficiency, working temperature
- Smaller form factor
- Option for energy regeneration

Figure 2: Principal trends for e-motor and traction inverter

Half bridge molded module benefits

STMicroelectronics is a pioneer in silicon carbide technology, especially for automotive applications. To address market challenges, it is developing a new family of molded half-bridge modules, with single-side and double-side cooling, addressing both 750V and 1200V breakdown classes with a current range up to 650A.

Benefits of power modules approach

- Flexible use of TSC or DSC
- Direct or indirect cooling
- Compact and scalable design approach
- Lower loop inductance
- Technology options:
    - 750V for 400V bus
    - 1200V for 800V bus

Figure 3: Key features of the new half bridge molded modules

Molded modules represent a step forward for traction inverters, enabling new power levels and system compactness. The half-bridge approach reduces stray inductance in the power loop by 40% compared to ACEPACK DRIVE (standard potted gel module).

Lower stray inductance enables higher di/dt and dv/dt, reducing switching losses while avoiding significant drain-source voltage overshoot during turn-off and drain-source current peaks during turn-on, as shown in Figures 10 and 11.

The $R_{THj\text{-}fluid}$, under the same conditions (T_{fluid} and coolant speed), is reduced by about 6.9% compared to ACEPACK DRIVE. This provides power designers with a higher power loss budget or the possibility to reduce cooling requirements and dimensions. Another benefit of molded modules is increased robustness against humidity and dust penetration compared to gel-potted modules, enhancing the application's reliability.

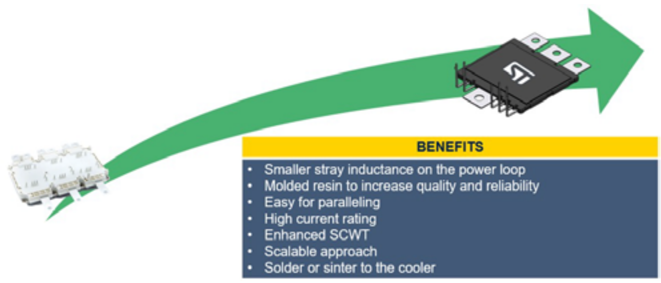

Figure 4: Benefit of molded modules

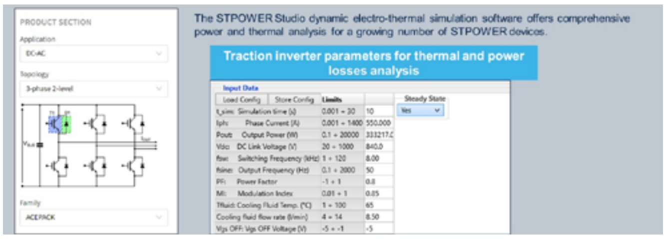

Figure 5: Power studio snapshot from website

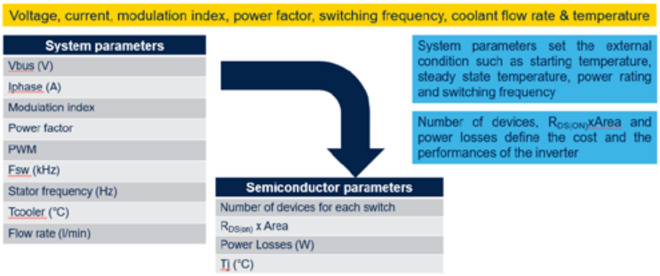

Figure 6: Application and device parameters

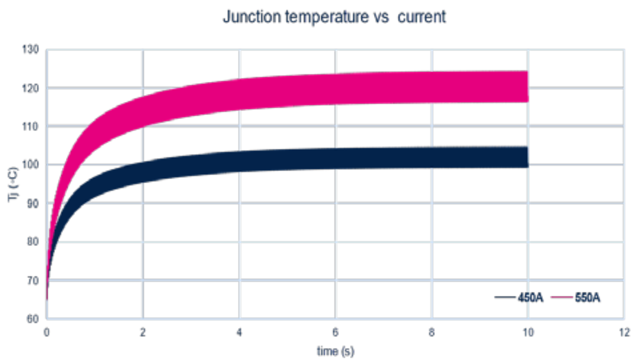

Figure 7: Junction temperature variation vs phase current at 850V

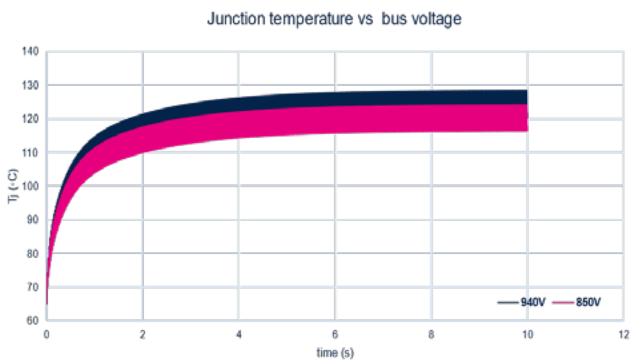

Figure 8: Junction temperature variation vs bus voltage at 550A

Finally, the half-bridge molded module allows sintering the power module to the cooler, typically reducing the $R_{THj\text{-}fluid}$ by about 15-20% compared to soldered attachments.

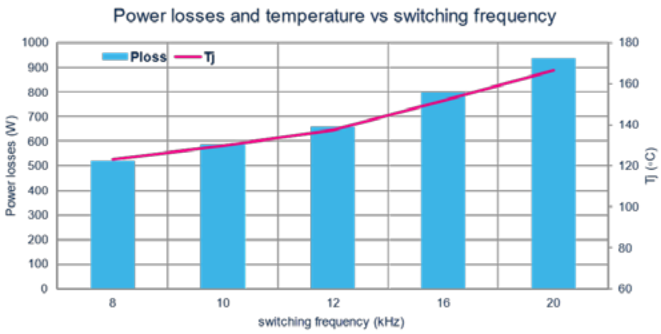

Figure 9: Power losses and Tj evolution vs switching frequency with 940V and 550A

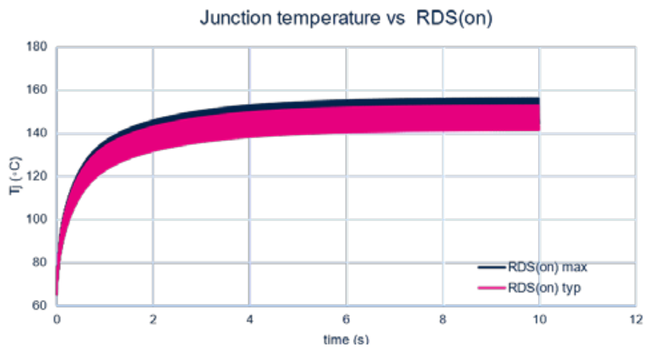

Figure 10: Junction temperature variation vs RDS(on) spread with 940V and 550A

Electrical and thermal evaluation

To validate the features of the molded half-bridge power module, a thermo-electrical analysis was performed, focusing on switching performance (both turn-on and turn-off) under different conditions for modern traction inverters. The analysis was conducted using Power Studio, an online tool provided by ST (https://eds.st.com/power-studio/).

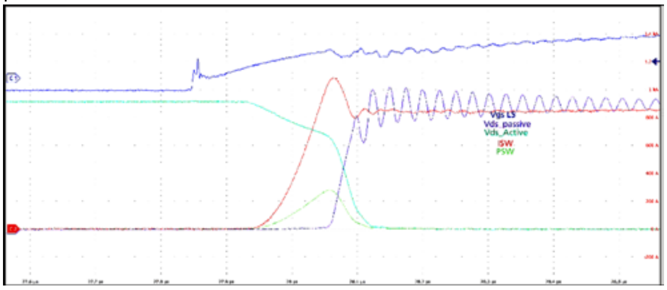

Figure 11: Waveforms during turn-on

I_{DSpeak_ON} 1050A	V_{DS} 850V	R_{G_ON} 6.8Ω
• V_{GS} DUT yellow, 10V/div • V_{DS} DUT red, 200V/div	• I_{DS} DUT light blue, 200A/div • P_{SW} DUT purple, 500kW/div	• V_{DS} passive device green, 200V/div

Power Studio allows designers to check power losses, and maximum and average junction temperatures using application and device parameters as inputs.

This enables the optimization of the number of devices, $R_{DS(on)}$, and the R_{TH} of the cooling system.

The new 1200V – 2.6 mΩ single-side molded module was evaluated in Power Studio.

Figures 7 to 10 show the results of several analyses considering key parameters in a traction inverter: phase current, bus voltage, switching frequency, and device $R_{DS(on)}$ spread. Power Studio allows designers to assess the impact of various conditions related to both application and device. It also checks if the operating point is within the maximum junction temperature, which for the selected power module is 175°C.

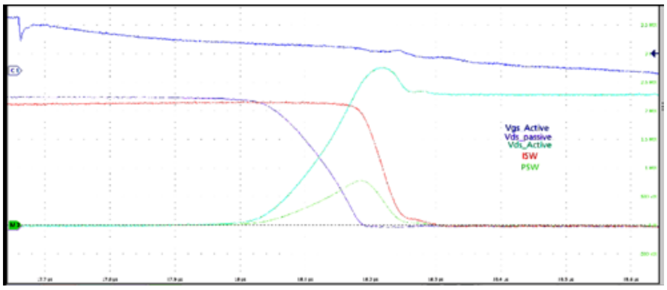

Figure 12: Waveforms during turn-off

I_{DS_OFF} 850A	V_{DSpeak} 1100V	R_{G_OFF} 12Ω
• V_{GS} DUT yellow, 10V/div • V_{DS} DUT red, 200V/div	• I_{DS} DUT light blue, 200A/div • P_{SW} DUT purple, 500kW/div	• V_{DS} passive device green, 200V/div

The selected power module can sustain high demanding requirements such as 940V, 550A, and 20 kHz without exceeding the maximum allowable junction temperature.

After the initial simulation evaluation, the module was tested on a double pulse test bench to evaluate switching performance in terms of commutation speed, switching energy, and noise.

Both turn-on and turn-off were evaluated (Figures 11 and 12). The low-side device is the DUT, while the high-side device is the passive device used as freewheeling. V_{GS} waveforms during turn-on and turn-off are clean without significant noise or ringing, despite lower gate resistance (6.8 Ω for turn-on and 12 Ω for turn-off). The maximum V_{DS} overvoltage during turn-off is well below the minimum breakdown voltage of 1200V, with a maximum value of 1100V.

The V_{DS} overvoltage margin is about 100V during turn-on on the passive device and 100V during turn-off on the active device, allowing further reduction in gate resistance to lower both turn-on and turn-off energies.

Conclusion

STMicroelectronics has developed a new family of transfer molded modules, both single-side and dual-side cooling, to meet the new BEV requirements in terms of power handling capability, electrical, and thermal performance. Equipped with the latest SiC technology, these modules push the boundaries of traction inverters, enabling new levels of performance while maintaining very low or zero noise during commutation. They also introduce a new concept of power density and power level.

www.st.com

Mitigating DC Link Antiresonance for WBG-based Designs

One basic requirement for DC link capacitors is the maximum ripple current they must carry. However, even with correct component selection for this rating, parts of the capacitor bank could become much hotter than calculated, especially in fast-switching converters with wide bandgap (WBG) semiconductors, leading to catastrophic failures in some cases. Responsible for this are hidden currents due to parasitic resonances. What causes this? How to mitigate it?

By Martin Neudecker, Global Sales Development Industrial & HA Application Specialist & Reference Design, TDK Europe GmbH , and Pradip Chatterjee, Principal Engineer, Infineon

By using silicon carbide (SiC) devices, AC-DC and DC-DC converters are rapidly evolving into systems with higher switching frequencies, efficiencies, and power densities. Because the voltage (du/dt) and current (di/dt) transients are more than ten times faster than in silicon devices, parasitic component effects become much more critical. As a result, the voltage overshoot is higher and ringing lasts longer. This can affect the service life of active and passive components.

A key functional block inside a typical converter is the DC link and all associated components. It often performs the following three functions:

- Providing energy storage capability for averaging the rectified mains voltage (grid frequency -50/60 Hz),
- handling the switching frequency (plus harmonics) ripple current caused by the switching devices (typical switching frequency -20 kHz to 150 kHz range) and
- providing a sufficiently low high-frequency commutation loop inductance to avoid an excessive voltage overshoot when high di/dt values are applied during switching (MHz range)

The first two functions are often accomplished by the same capacitors in terms of technology. For the last function, an additional low-inductance component is often required, which typically has a low capacitance and must be placed next to the power semiconductors. Especially for converters with wide bandgap semiconductors, these become more and more important due to the high di/dt values.

Usually, one capacitor technology handles the low-frequency part (L_F) and thus the first two tasks and is named C_{LF} in the following. The other is for the high-frequency portion (H_F) and is called C_{HF}. Since C_{LF} is much higher in capacitance than C_{HF} and therefore mechanically much larger, long interconnection structures are usually involved in between. This results in this equivalent circuit diagram (Figure 1).

Although a laminated busbar, for example, can minimize the parasitic inductance of the interconnect structure ($L_{parasitic}$) this must always be carefully considered when analyzing the capacitive function block of the whole converter.

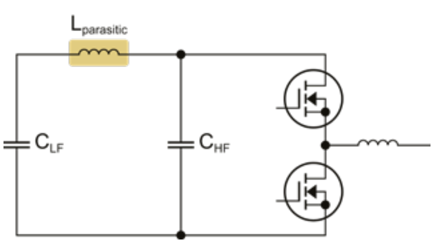

Figure 1: Equivalent circuit of the commutation loop with the parasitic inductance of the interconnection structure $L_{parasitic}$

Simplified equivalent circuit

For a better understanding of the mechanism of antiresonance, certain aspects can be simplified.

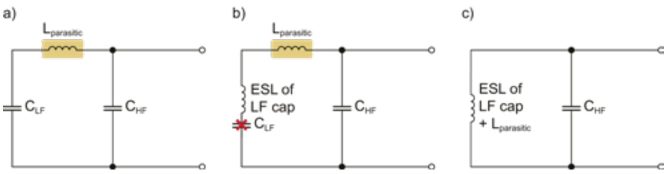

Figure 2: Equivalent circuits: a) LF and HF capacitor portions in parallel with parasitic L of the interconnection structure. b) LF capacitor in detail (i.e., C and ESL in series) with C being neglected. c) Resulting simplified equivalent circuit at antiresonance frequency; ESL and parasitic L summed up

Taking the parallel configuration of the LF and HF capacitors as a starting point, the interconnection structure has a certain parasitic inductance ($L_{parasitic}$; Figure 2a). Since the frequency range of interest is usually above the (series) self-resonant frequency of the LF capacitors, it can be substituted by the ESL only, without considering the capacitive component (see Figure 2b). On the other hand, the frequency range considered is usually well below the self-resonant frequency of the HF capacitors, so they can be approximated by their capacitive part only, without considering the ESL. Finally, the ESL of the LF capacitors and the parasitic L value of the interconnect structure can be summed to a single inductance, resulting in the simple LC parallel resonant circuit shown in Figure 2c. This will approximate the response of the entire circuit of LF and HF capacitors in the frequency domain of its impedance peak. This parallel resonant tank phenomenon is known as antiresonance.

For this simplified equivalent circuit, the resonant frequency can be determined as follows:

$$f_{res} = \frac{1}{2\pi \cdot \sqrt{(ESL_{LF} + L_{parasitic}) \cdot C_{HF}}}$$

At this antiresonance frequency, the impedance of the circuit rises (significantly) above the expected value compared to when the impedance of the individual elements is considered separately.

For simplicity, the equivalent series resistances (ESR) of the components were not considered in the following analysis. In general, however, a higher ESR means a lower quality factor of the resonant circuit, so that the resonance is wider and flatter, and vice versa.

At this stage, it is most important to understand that three crucial reactive elements determine the antiresonance frequency:

- the resulting ESL of the LF capacitor bank,
- the inductance of the interconnection structure between the HF and LF capacitors, and
- the capacitance of the HF capacitors.

Calculation examples

Two examples – one not optimized and one optimized – will be simulated using the simplified equivalent circuit diagrams (Figures 3 to 5). Subsequently, the optimized example will also be measured in a real system. In the simulation, the impedance measurement takes place at the point where the semiconductor switches are connected in the real system (I1 is used here for the impedance measurement).

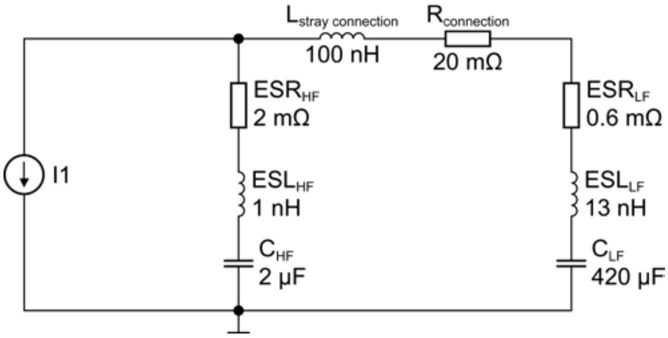

Figure 3: Equivalent circuit diagram of the highly inductive DC-link circuit

In the first, not optimized example (Figure 3), three LF capacitors of 140 µF each (total C_{LF} = 420 µF) are connected in parallel, each having an ESL_{LF} of 40 nH (total approx. 13 nH) and an ESR_{LF} of 0.6 mΩ. In this case, the busbar is poorly designed, resulting in a total inductance ($L_{stray\_connection}$) of 100 nH. At the same time, some may be concerned about having enough HF capacitors, so a total of 2 µF is used as C_{HF}. The frequency curve in Figure 4 shows an impedance peak at about 330 kHz that cannot be explained by the impedance curves of the individual capacitors only. This peak is the so-called antiresonance of the overall circuit.

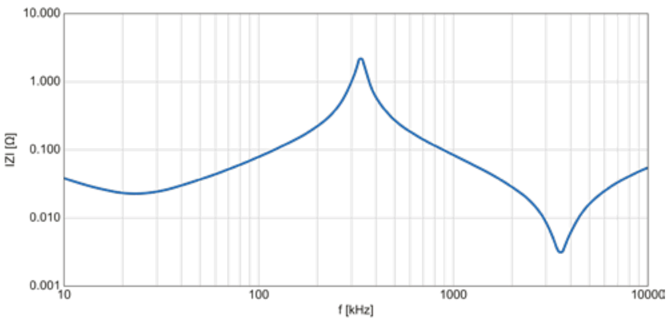

Figure 4: Frequency curve for the highly inductive DC-link circuit

For example, if a resonant converter is attached to such a design and operated at about 110 kHz, which is not a big challenge for resonant SiC topologies, the strong third harmonic of the ripple current at 330 kHz would fully hit the impedance peak of this poorly designed DC link. In this case, resonant currents are likely to circulate between the capacitors C_{HF} and C_{LF} and the parasitic inductances (see Figure 3) that are much higher than the harmonic of the ripple current itself. This can cause the capacitors to overheat and even fail as this resonant current causes additional losses at the ESR ($I^2 \cdot R$).

This example illustrates how harmful antiresonances can become and how important it is to ensure a proper RF design even in the so-called low-frequency portion of such mixed DC link capacitor assemblies.

In the second, optimized example (Figure 5), the LF capacitors are exactly the same as in the first one, but close attention was paid to a low-inductance design. The busbar has a leakage inductance of 20 nH and an ESR of 25 mΩ. The HF capacitor bank has a total of 1 µF (C_{HF}), an ESL_{HF} of 2 nH, and an ESR_{HF} of 4 mΩ.

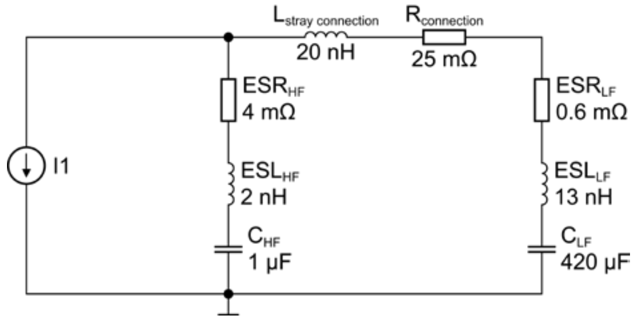

Figure 5: Equivalent circuit diagram of the low-inductance DC link

Here, the impedance peak is located at about 850 kHz, a much higher frequency than in the first example (Figure 6).

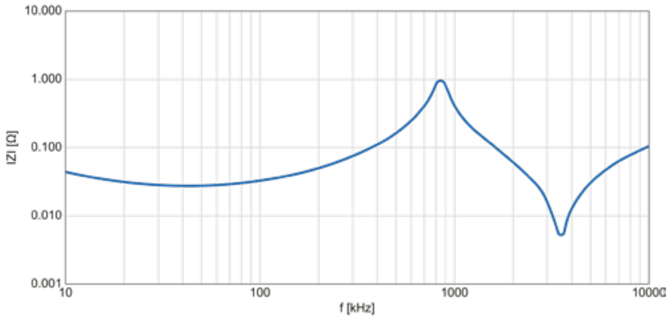

Figure 6: Frequency curve for the low-inductance DC link

Mitigating the antiresonance effect

Based on the three critical factors that determine the antiresonance frequency, there are strategies for dealing with the issues caused by antiresonance:

- **Shift the antiresonance frequency to higher frequencies.** This can be achieved primarily by reducing the ESL of the LF capacitors and any parasitic inductance in the interconnect structure. Keep in mind that the lower capacitance values of the HF capacitors or snubbers can also contribute to this. The goal of this strategy is to ensure that the antiresonance is not hit by the ripple current or by low-order harmonics with their higher power levels.
- **Move the antiresonance frequency below the switching frequency.** The objective of this strategy is also to ensure that the antiresonance is not stimulated by the ripple current at all. To move the frequency of the antiresonance this far, an additional choke is often inserted between the LF and HF capacitors. This increases the inductance of the interconnect structure significantly. Additionally, it may also be useful to massively increase the capacitance of the HF capacitors.
- **Set all switching frequencies of the system and their harmonics outside the critical antiresonance frequency band.** Attention must be paid to the tolerances and aging behavior of the passive components in the DC link as their values may vary and thus directly affect the antiresonance frequency. Sometimes this strategy proves impossible, for example when the switching frequencies vary over a wide range during operation, such as in resonant topologies.
- **Selective attenuation of the antiresonance impedance peak.** This theoretical option adds a resistive element to the circuit that is effective only in the relevant frequency range and does not unduly affect the regular ripple current. Such a mechanism could, for example, use the skin effect in the interconnect structure, since its resistance increases with frequency. This strategy could

CoolSiC™ MOSFET 400 V Generation 2

Unique combination of performance, reliability and ease-of-use

SiC MOSFET optimized for 400 V breakdown voltage

- Highest efficiency and power density
- System cost/performance optimization
- Fast-switching capability
- Low EMI
- Easy unipolare gate driving
- Perfect fit to single, 2-level and 3-level topologies

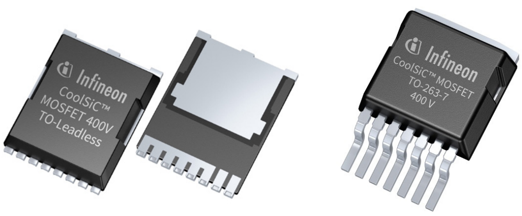

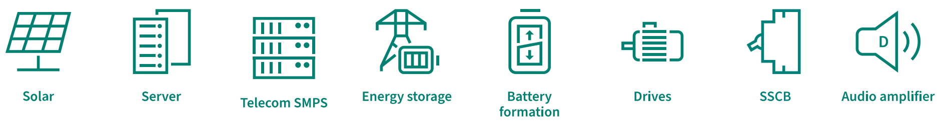

Click here for more information.

be promising in combination with the first strategy mentioned above. Further research on this topic is still needed to prove it and provide practical design guidance for it.

Keep in mind that the ESR of aluminum electrolytic capacitors usually decreases significantly with temperature. Therefore, a converter that works perfectly at +25 °C may exhibit antiresonance at higher temperatures.

Double pulse test as metrological verification

With a double pulse test, the antiresonance oscillation can also be determined directly from the voltage waveform. Figure 7 shows the equivalent circuit of the double pulse test of a C_{HF}/C_{LF} structure with the parasitic elements. These include the ESLs of C_{LF} and C_{HF}, the inductance of the interconnect structure ($L_{parasitic}$), the parasitic inductance of the busbar or PCB between C_{HF} and the devices ($L_{stray\ connection}$), the parasitic inductances of the drain and source terminals of the devices (L_D, L_S), the parasitic capacitance of a free-wheeling diode (C_{DD}), the equivalent parallel capacitance of the inductive load (C_{EPC}), and the parasitic inductance of the meter (L_{sense}). The gate loop includes the parasitic inductance of the gate (L_G) and the source terminal (L_S). Also, the parasitic capacitances in the MOSFETs (C_{GD}, C_{GS}, and C_{DS}) must be considered.

It is particularly important to note that the measurement continues after the second pulse has been turned off. Here, both components are off, but the body diode of the upper switch is still conducting, driven by the coil current (green arrow in Figure 7). Therefore, the DC link voltage (plus the nearly constant voltage drop of the body diode) is also visible at the switching node during this time. This means that voltage oscillations, especially between C_{HF} and C_{LF}, can be easily detected at the switching node even in this operating state. In the case of an antiresonance oscillation, high currents flow back and forth between C_{HF} and C_{LF} (red arrows in Figure 7).

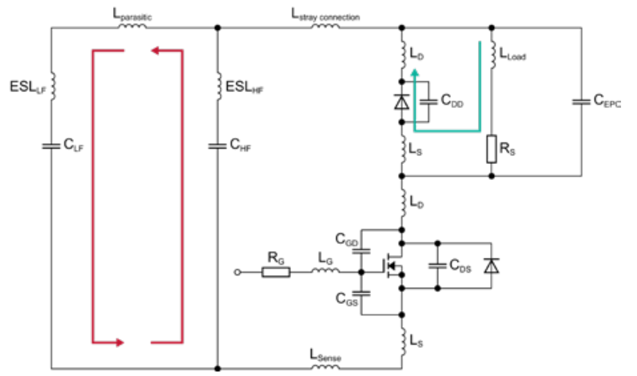

Figure 7: Equivalent circuit diagram of a double-pulse test setup with parasitic elements as well as the free-wheeling current (green arrow) and the antiresonance current (red arrows)

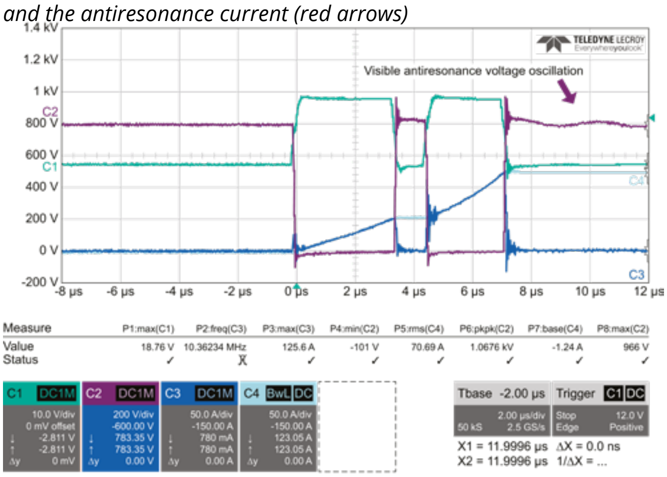

Figure 8: FF8MR12W2M1P_B11 double pulse test with the unoptimized example; in violet the voltage at the switching node oscillates with an antiresonance frequency around 400 kHz

Although C_{HF} has a low impedance at the typical antiresonance frequencies, the large oscillating currents can cause voltage oscillations across this capacitor, which can be observed at the switching node (Figure 8).

Results with a 50 kW EV charger test setup at Infineon

Figure 9 shows the power conversion board of a 50 kW EV charger test setup where the antiresonance issue described above was solved. For this purpose, the busbar ($L_{parasitic}$) was optimized together with the C_{HF} values to reduce the oscillating currents in the loop. Multiple parallel terminals of the busbars help to reduce the effective inductance ($L_{parasitic}$) in the path. Knowing the natural resonant frequency of this resonant circuit helps the designer select the proper switching frequency of the converter. Stimulating the natural resonant frequency by harmonics of the switching frequency should be avoided.

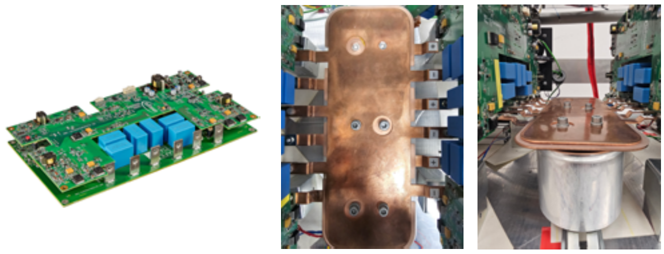

Figure 9: On-board CHF and multi-terminal busbar on an Infineon power conversion board for DC EV chargers

The oscillogram (Figure 10) shows a waveform example after design optimization. The voltage at the switching node is the light blue curve and shows an antiresonance oscillation with a frequency of about 1 MHz over a time of some 1 µs.

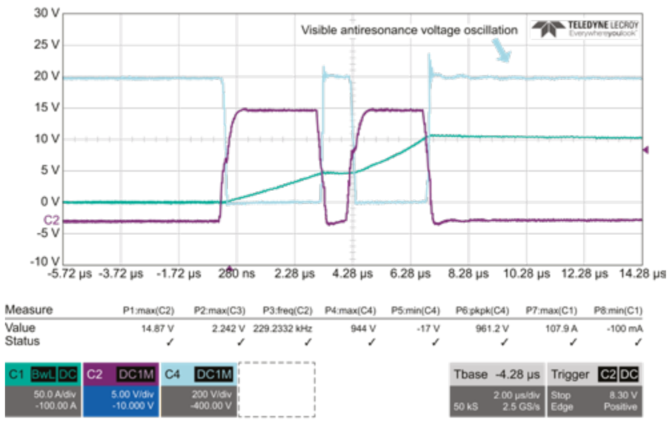

Figure 10: FF8MR12W2M1P_B11 double pulse test with the optimized 50 kW power converter test setup by Infineon

Conclusion

Power system designers should thoroughly investigate antiresonance issues early in the development process to avoid serious, unanticipated degradation of power converters in later design phases and even failures during operation. Choosing the right switching speed and frequency for the power converter, properly designing the commutation loop, including the busbar, and properly selecting the reactive components, such as the HF and LF capacitors, appropriately can mitigate a catastrophe before it happens.

www.us.lambda.tdk.com/applications/emi-solutions

Reliable Switching Power Supplies: Overvoltage and Avalanche Energy in MOSFETs

Why do switching transistors fail in the event of an overvoltage, even though the energy appears to be well below the specified avanlanche energy? This article shares practical experiences and proposes explanations based on the example of a flyback converter.

By Prof. Markus Rehm, Power Supply Expert, and co-author Sean Carthy, PhD, InducAce Ltd.

Overvoltage on the switching transistor is the most frequent cause of failure in my fault analyses. This has not changed in the last 25 years, although today's MOSFETs should be much more robust than the earlier bipolar transistors according to the datasheet. Many MOSFETs have an "avalanche energy rating". In the event of an overvoltage, they do not fail immediately, but the specified amount of energy must first be exceeded before the avalanche effect is triggered.

For many switching power supply developers, this seems to be a great feature because they no longer have to look so closely at the voltage peaks. Whether at maximum mains voltage, during start-up or in the event of a short circuit, if the energy of the overvoltage is significantly below the specified datasheet value, you can apparently proceed with blind confidence. From my experience, that would be a fatal mistake!

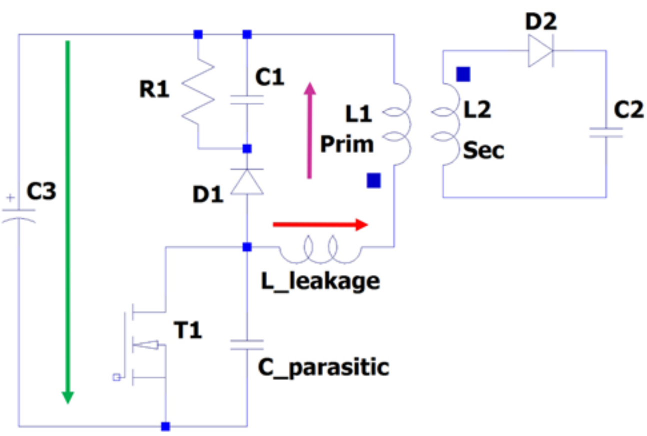

Figure 1: Flyback converter principle with leakage inductance and R-C-D snubber network.

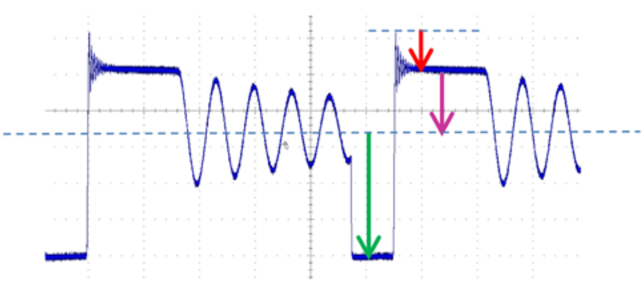

Figure 2: Typical drain voltage curve on the switching transistor of a flyback converter.

Where does the overvoltage come from?
The culprit is clear and easy to identify: it is the parasitic inductance $L_{leakage}$, which is not demagnetised via the freewheeling diode D2 during the transfer time. The energy stored in it (½ $L_{leakage}$ I^2) is transferred to the existing parasitic capacitance and generates an overvoltage there (½ $C_{parasitic}$ V^2). If there were no parasitic capacitance, the voltage would rise to infinity. The resultant MOSFET voltage is greatest in the flyback converter (see figure 1), because the overvoltage is superimposed on the "shoulder voltage".

Due to the air gap in the transformer and the freewheeling diode situated on the secondary side, the leakage inductance is very high with this topology. The junction capacitance of the switching transistor is low, and this results in a high overvoltage peak (figure 2). However, regardless of the topology, there is always some leakage inductance due to the leads and vias.

How do you measure this overvoltage correctly?
It is difficult to measure this overvoltage peak correctly because it is reduced by the effect of the probe capacitance. In addition, the peak is sometimes only a few nanoseconds long and the properties (bandwidth, resolution, memory depth) of the overall probe and oscilloscope system are often not sufficient. It is interesting to note that measurements made by three different engineers using their own equipment on the same power supply yielded drain voltage values between 710 V and 850 V! In the case of a 750 V MOSFET, this can be the difference between life and death!

Do you need a snubber network?
We only measure a power supply sample at room temperature. The overvoltage peak depends on parasitic element properties whose values are poorly specified, and which also have large tolerances and are temperature dependent. For this reason, a snubber on the switching transistor is recommended to mitigate fluctuations occurring in production quantities. For the flyback converter, I consider a classic "R-C-D snubber" (figure 1) the optimum solution in terms of reliability. The capacitor absorbs the energy of the leakage inductance, the resistor discharges it for the next cycle and the diode ensures a low-impedance circuit in the "charge" direction and brings the resistance into the circuit in the "discharge" direction to minimize losses in the switching transistor when it is switched on. That means the snubber diode serves as a freewheeling diode for the leakage inductance and should therefore be as close as possible to the drain of the MOSFET. Alternatively, you could use a single capacitor or an R-C element, or a robust TVS diode that absorbs the voltage spike. Unfortunately, a snubber costs money and space and increases power losses.

What do "avalanche energy" and "avalanche current" mean for MOSFETs?
If an overvoltage occurs in the semiconductor, a first electron is knocked out of its bond and this knocks out further electrons. This leads to an avalanche effect which destroys the component. For

MOSFETs with an avalanche energy rating, a certain threshold of energy must first be exceeded before the avalanche effect is triggered. This energy is specified in the datasheet of a MOSFET.

In the case of the ST45N65 the avalanche energy rating is exactly 810mJ at a junction temperature of 25 °C (figure 3). This value is of course completely irrelevant – which switching transistor is operated at 25 °C? The avalanche energy at 110 °C would be far more pertinent, for example. This would be important to know but is not specified in the datasheet.

Table 2. Absolute maximum ratings

Symbol	Parameter	Value: D²PAK TO-220	Value: TO-220FP	Unit
V_{GS}	Gate-source voltage	± 25		V
I_D	Drain current (continuous) at T_C = 25 °C	35	35 (1)	A
I_D	Drain current (continuous) at T_C = 100 °C	22	22 (1)	A
I_{DM} (1)	Drain current (pulsed)	140	140 (1)	A
P_{TOT}	Total dissipation at T_C = 25 °C	210	40	W

Table 4. Avalanche characteristics

Symbol	Parameter	Value	Unit
I_{AR}	Avalanche current, repetetive or not repetetive (pulse width limited by T_{jmax})	9	A
E_{AS}	Single pulse avalanche energy (starting t_j=25°C, I_d= I_{AR}; V_{dd}=50)	810	mJ

Figure 3: Extracts from the STF45N65 datasheet.

This MOSFET from ST can pulse 140 A and yet the avalanche current is specified as 9 A (figure 3). The current is the same in the main inductance and leakage inductance and it continues to flow into the MOSFET after it is switched off. Who operates a 140 A MOSFET at 9 A?

Infineon specifies this better. In the 600 V CoolMOS datasheet for the IPL60R185P7, the avalanche energy is specified as a function of temperature (figure 4).

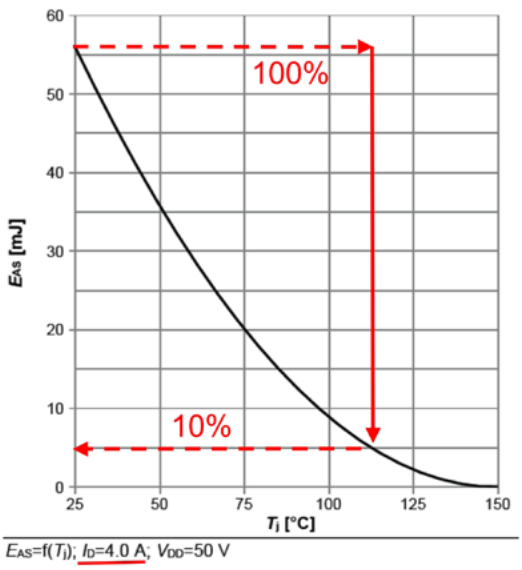

Figure 4: Avalanche energy as a function of the junction temperature (datasheet extract IPL60R185P7).

The graph shows that at a junction temperature of 110 °C only 10 % of the original value of 25 °C remains, i.e. only 5 mJ instead of the original 55 mJ.

Unfortunately, the MOSFET temperature can only be measured on the outside of the housing and only integrated over time. In fact, the actual temperature on the chip pulses with the switching frequency depending on the switch-on, conduction and switch-off losses as well as the transient thermal impedance. This can be simulated with LT-Spice, for example. We therefore do not know exactly how high the actual chip temperature is when the overvoltage pulse occurs. In any case, it is higher than measured at the housing. When the MOSFET blocks, the junction cools down. If we have zero voltage switching, then there are no switch-on losses. As soon as the current flows, the conduction losses increase quadratically with the current (I^2 x R_{DSon}) and the chip heats up quickly. When switching off, there are large switch-off losses and the chip becomes hot. And this is precisely when the overvoltage peak occurs and precisely when we need to know the junction temperature in order to be able to read off the avalanche energy that is still permitted in the diagram!

According to its datasheet, this above-mentioned power MOSFET from Infineon can handle a pulse current of 53 A. So it will probably not be operated with only 4 A. However, the avalanche energy is specified with precisely that value of 4 A – according to the small print on the left below the diagram (figure 4). The maximum permissible avalanche current is also specified as 4 A in the datasheet (figure 5). This means that we should not actually operate the 53 A MOSFET with more than 4 A if we want to utilize the avalanche energy, and this only applies at 25 °C!

1 Maximum ratings
at T_j = 25°C, unless otherwise specified

Table 2 Maximum ratings

Parameter	Symbol	Values: Min.	Values: Typ.	Values: Max.	Unit	Note / Test Condition
Continuous drain current[1)]	I_D	- -	- -	19 12	A	T_C=25°C T_C=100°C
Pulsed drain current[2)]	$I_{D,pulse}$	-	-	53	A	T_C=25°C
Avalanche energy, single pulse	E_{AS}	-	-	56	mJ	I_D=4.0A; V_{DD}=50V; see table 10
Avalanche energy, repetitive	E_{AR}	-	-	0.28	mJ	I_D=4.0A; V_{DD}=50V; see table 10
Avalanche current, single pulse	I_{AS}	-	-	4.0	A	-

Figure 5: Maximum ratings (datasheet extract IPL60R185P7).

In the case of avalanche energy, we have seen that at 110 °C only 10 % of the value of 25 °C is permitted. Unfortunately, there is no diagram for the Avalanche current as a function of temperature. We can only hope that the derating is not 10 % at 110 °C, as with the Avalanche energy, otherwise only 400 mA would be permitted!

How do MOSFET manufacturers specify the avalanche energy rating?

Let's look at how almost all MOSFET manufacturers measure and determine the avalanche energy, using Infineon as an example. Before the test, the MOSFET is connected to 50 V via the coil and free from stress at 25 °C! In the real power supply unit, the MOSFET is at 300 V to 400 V before switching on and at 500 V in the "off" state, so you already have leakage currents of up to almost 1 mA and corresponding losses. In addition, the MOSFET in the power supply unit constantly switches currents on and off at a high frequency and its temperature might be 100°C or higher.

In the test, however, the MOSFET is only switched on once and then allowed to conduct until the specified current (e.g. 4 A) is reached. The test circuit (figure 6) is similar to a boost converter, but without a freewheeling diode to demagnetize the inductance. As soon as the MOSFET switches off, the drain voltage increases indefinitely and is then only clamped by the MOSFET to a value V(BR)DS that is somewhere above the maximum permissible reverse voltage. This can often be seen in the measurement by a plateau that suddenly limits the oscillation. In the test, the MOSFET then remains off forever and is at 50 V.

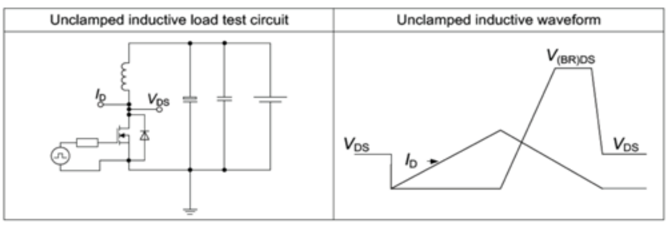

Figure 6: Datasheet extract for the avalanche energy test.

In an application note from Infineon [2] on the subject of "Avalanche Energy", you can see an oscilloscope diagram (figure 7) which shows that the MOSFET conducts for 40 µs (current ID rises) and demagnetization takes 22 µs (current ID falls). The avalanche energy therefore has 22 µs to distribute itself in the chip.

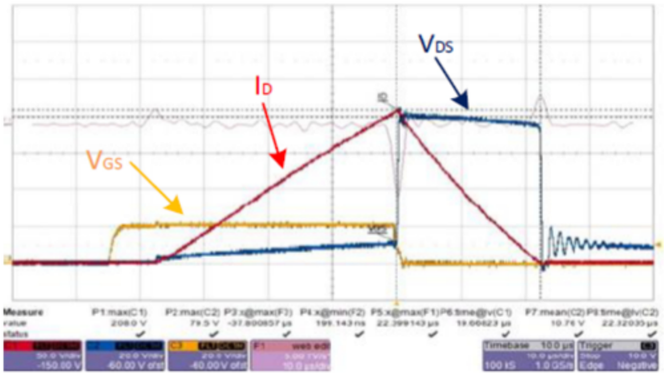

Figure 7: Datasheet extract for the avalanche energy test

In an application note from Vishay [3] I read another very interesting aspect (figure 8): "Typical modern power MOSFETs have millions of identical trenches, cells or many strips in parallel to form one device... For robust designs, then, the avalanche current must be shared among these cells/strips evenly."

Typical modern power MOSFETs have millions of identical trenches, cells or many strips in parallel to form one device, as shown in figure 7. For robust designs, then, avalanche current must be shared among many cells/strips evenly.

Figure 8: Extract from an application note from Vishay

In this Vishay application note there is also an oscillogram showing that the demagnetization of the inductance and thus the overvoltage lasts 70 µs.

Durations of 22 µs or 70 µs are irrelevant – the overvoltage in the power supply lasts a tiny fraction of those times, between 5 ns and 500 ns. The avalanche current must therefore be distributed evenly across the millions of parallel structures in a hundredth to a thousandth of the time specified in the datasheet, in order to achieve a "robust design". This means that not only the chip-internal resistors but also inductances play a major role. As far as I know, MOSFET manufacturers do not test this scenario – and if they don't test it there is a strong chance that they don't optimize the design for it either.

In addition, there are often many voltage peaks in succession, whether during start-up, mains interruption, mains surge voltage or in the event of an overload or short circuit. In some datasheets, the value for "repetitive" can also be found alongside "Single Pulse Avalanche Energy". For the Infineon Coolmos device mentioned above (figure 5), the "repetitive" value is only 5 % of the "single pulse" and has the same unrealistic test conditions.

The datasheet for the avalanche energy often specifies "gate voltage zero" as a condition. Take a close look at your oscilloscope measurement: During the voltage peak on the drain, the gate voltage is often clearly positive, one volt or more, due to the miller effect and an imperfect gate driver circuit.

Consider or ignore avalanche energy?

Based on these findings and considerations, the question arises as to whether the specified avalanche energy should be taken into account at all. The answer is clear for me, and it is "NO!" The maximum permitted drain voltage applies and this must not be exceeded in any operating case. For me, this is an important prerequisite for getting a reliable power supply unit.

The MOSFET manufacturers basically say the same thing: "The maximum ratings must be strictly adhered to, even for short torques, because otherwise the service life and reliability of the MOSFET cannot be guaranteed."

We power supply developers test our circuit and if nothing breaks, then we give it the thumbs up. But if only one hundred of these millions of parallel structures break, we won't even notice. The quality department may carry out a thousand tests, but even then we don't notice that a hundred thousand structures are broken because there are still millions intact. There's a lot of guesswork when the customer's device fails a year or more later, everything had been calculated and tested and found to be good.

Conclusion

The maximum reverse voltage of a MOSFET is specified in the datasheet. Many MOSFET manufacturers warn against exceeding this maximum permissible reverse voltage, even for a brief moment, so as not to impair the service life and reliability.

If an avalanche energy is specified in the datasheet, then this will not correspond at all to the real application in the switching power supply. The avalanche current is much higher, the temperature is much higher, the overvoltage peaks will always be repetitive. In addition, the avalanche energy in the power supply must be distributed evenly over the millions of parallel structures in the chip in a thousandth of the time specified by the MOSFET manufacturer. It doesn't help if some manufacturers test 100 % of the avalanche energy in production. Even extensive long-term testing in the power supply unit only provides deceptive certainty, because the semiconductor may only be damaged a little more with each test and then only fail at the customer's premises after a year of operation.

My recommendations:

1. Stay below the maximum specified reverse voltage in all operating conditions.
2. The more uncertain you are about the accuracy and reproducibility of your measurement, the more margin you should allow.

These recommendations apply not only to switching transistors in AC/DC converters on the primary side, but also to synchronous rectification on the secondary side, half bridges in DC/DC converters and Schottky diodes with avalanche ratings.

By the way: This report will be added to the one-day seminar "Reliable power supplies" for future presentations. [1]

Sources:

[1]: Rehm, Markus; Seminar "Reliable Power Supplies"
[2]: Infineon AN_2304_PL18_2305_004059
[3]: Vishay Siliconix AN-1005

About the Authors

Prof. Markus Rehm runs a power electronics laboratory, supporting his customers with research, development and consulting services for over 25 years. He enjoys sharing his extensive experience at conferences and seminars. He has been a lecturer at Furtwangen University since 2008 and was appointed honorary professor in 2019.

Co-author is Sean Carthy, PhD, InducAce Ltd. Sean has 40+ years experience in power electronics as a designer, manager and consultant and started his own consultancy, InducAce Ltd in 2009. He particularly enjoys the challenges of on-site troubleshooting and has worked in the consumer, industrial, automotive, railway, medical and catering equipment markets.

www.ib-rehm.de

Applications and Use of EMI Filters for Industrial and Medical Applications

In today's technologically driven world, electronics play a pivotal role in our daily lives. From smartphones to industrial machinery, the abundance of electronic devices has led to an increased need for effective Electromagnetic Interference (EMI) and Electromagnetic Compatibility (EMC) filtering. These filters ensure that electronic devices function harmoniously without causing or being affected by unwanted electromagnetic emissions. By exploring fundamental EMI/EMC concepts, regulatory considerations, and practical applications, we can provide a comprehensive understanding of the importance of EMI filtering in our increasingly electronic world, along with some guidance for engineers on selecting the right filters for their specific needs.

By Tom Tillman, Director of Marketing, TDK-Lambda Americas

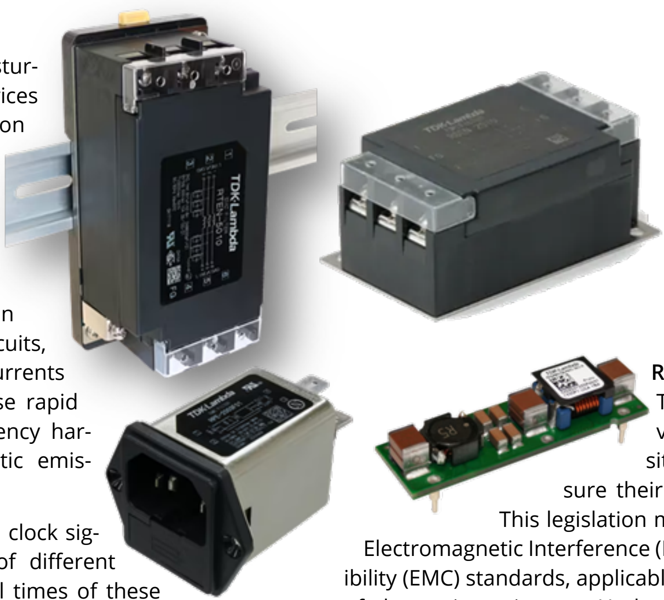

Understanding EMI and EMC

Emissions are electromagnetic disturbances generated by electronic devices that can interfere with the operation of other devices. These disturbances can be caused by numerous factors. The following are examples of common sources of electromagnetic interference.

Switching Transients: Common in power supplies and digital circuits, switching transients occur when currents or voltages change abruptly. These rapid changes can generate high-frequency harmonics, leading to electromagnetic emissions.

Clock Signals: In digital electronics, clock signals synchronize the operation of different components. The fast rise and fall times of these signals can produce significant harmonic content, contributing to emissions.

Functional Electromagnetic Fields: Motors, transformers, and other inductive components generate electromagnetic fields as part of their normal operation. When these fields fluctuate, they can induce currents in nearby conductive paths.

Signal Harmonics: Non-linear elements in a circuit, such as diodes and transistors, can distort signals, creating harmonics that extend into the radio frequency range. These harmonics can radiate or be conducted away from the device, causing interference.

It is also important to understand some of the key terminology distinctions associated with the study of EMI and EMC:

- *EMI vs. EMC:* Electromagnetic Interference (EMI) refers to the disruptive electromagnetic energy emitted by a device, while Electromagnetic Compatibility (EMC) is the ability of a device to function properly in its electromagnetic environment without causing or being affected by EMI.
- *Emissions vs. Immunity:* Emissions are the electromagnetic energy generated by a device, which can potentially interfere with other devices. Immunity, on the other hand, is the ability of a device to withstand external electromagnetic disturbances without degradation in performance.
- *Radiated vs. Conducted:* Electromagnetic Emissions can be either radiated, meaning they propagate through air or space, or conducted, meaning they travel along conductive materials like wires or cables. Each type of emission requires specific mitigation strategies to prevent interference.

Regulatory Considerations

The proliferation of electronic devices in modern society has necessitated stringent legislation to ensure their safe and harmonious operation. This legislation mandates compliance with specific Electromagnetic Interference (EMI) and Electromagnetic Compatibility (EMC) standards, applicable to manufacturers and designers of electronic equipment. Understanding these regulatory implications is crucial, as non-compliance can lead to legal repercussions, product recalls, and damage to a company's reputation.

Regulatory requirements for EMC compliance can vary by region, making it essential for manufacturers to understand and adhere to the standards specific to each market in which they operate. For instance, products sold in the European Union must comply with the EMC Directive (2014/30/EU), while those in the United States must meet FCC regulations.

Many regulations require that manufacturers certify their devices against the applicable regional requirements through a recognized or authorized third party evaluator. Even in regions where supplier self-declarations are technically permissible, it is usually wise to seek third party evaluation as a demonstration of due diligence.

Applications for EMI Filters

Stand-alone EMI filters play a vital role in enhancing the performance and reliability of complex systems across industrial and medical sectors. Let's take a closer look at some common applications in these spaces.

1. Power Supplies and Power Systems:
   In both industrial and medical environments, power supplies must be able to provide consistent, stable electrical energy. EMI filters are needed to prevent grid disturbances from propagating

to downstream equipment that may not tolerate it, and at the same time ensure that high frequency energy produced by the switch mode power conversion does not propagate upstream out onto the grid where it could potentially disrupt other off-line equipment nearby. EMI filters in power systems are crucial for eliminating noise that can cause disruptions in sensitive equipment, leading to errors or failures. For instance, in precision manufacturing, even minor power quality issues can result in significant production defects.

2. Rotating Machines
   Much of the world's total electrical load is comprised of rotating machines. Pumps and motors are key components in most of our higher powered devices such as house-hold appliances like air conditioners, refrigerators and laundry machines, or industrial devices like elevators, escalators, automated production machines or laboratory instruments like centrifuges. EMI filters contribute to device longevity by preventing premature wear and tear caused by electrical noise. In applications like CNC machines or robotic arms, this translates to smoother operation and reduced maintenance costs. Motors and pumps are also notorious for inducing electrical noise in nearby equipment. This noise is typically generated by the switching actions of the motor's control circuits, such as those found in variable frequency drives (VFDs), and by the commutation process in the case of brushed motors. The rapid switching of currents and voltages can produce electromagnetic interference (EMI) in the form of both conducted and radiated emissions.

3. Transmitting Devices
   In industrial communications equipment, EMI filters are pivotal in preserving signal integrity. They ensure that data transmitted between sensors, PLCs, and control systems is accurate and free from corruption. This is particularly crucial in automated processes where real-time data exchange is essential for coordination and efficiency.

4. Renewable Energy Systems
   In renewable energy systems, power inverters and DC to DC converters play a key role integrating solar or wind power into the grid. Much like with power supplies, the switch mode power conversion networks within these devices can generate strong electromagnetic fields that can manifest as both radiated and conducted emissions. These fields are the result of the high speed switching action of transistors creating rapid voltage and/or current discontinuities which contain a wide spectrum of frequency components, including high-frequency harmonics, which can interfere with the operation of nearby electronic equipment.

5. Industrial Machinery
   EMI filters in industrial machinery contribute to overall system integrity. They help in ensuring that the electromagnetic noise generated by the machinery does not compromise the accuracy of control systems or sensor readings. This is critical in processes like precision machining or automated assembly, where even small errors can lead to significant quality issues.

6. Medical Applications
   The medical care environment introduces several unique risks and challenges with regard to Electromagnetic Interference (EMI) and Electromagnetic Compatibility (EMC) due to the critical nature of medical devices and the sensitivity of the patients.

The foremost concern in the medical care environment is patient safety. EMI can lead to malfunctions or inaccurate readings in medical devices, which can have dire consequences, such as incorrect diagnoses, inappropriate treatments, or even life-threatening situations. The care environment introduces a potential conflict between several devices that are both extremely noise-sensitive and extremely noisy. Many medical devices are highly sensitive to electromagnetic fields. For example, devices like pacemakers, defibrillators, and neurostimulators can be affected by EMI, potentially leading to incorrect operation or failure. However, hospitals and clinics often have a high density of electronic equipment, including MRI machines, X-ray machines, CT scanners, and various wireless communication devices capable of generating strong electromagnetic fields. This creates a complex environment, increasing the potential for EMI.

Manufacturers need to take additional precautions in the design of EMC filters for medical applications as the safety features of the filters themselves are also held to a higher standard. These filters must exhibit constructional features such as increased isolation levels and lower leakage currents.

Because of these risks, medical devices are subject to stringent regulatory standards for EMC to ensure their safe and effective operation. Compliance with these standards can be challenging, given the diverse range of devices and the dynamic nature of the medical care environment. The medical care environment is constantly evolving, with new technologies and devices being introduced regularly. This dynamic nature requires ongoing assessment and management of EMI and EMC risks to ensure the continued safety and effectiveness of medical devices. The selection of suitable EMI and EMC filters for these applications is paramount to product success.

Filter Selection

Selecting the right EMI filter is a critical decision that hinges on understanding the specific needs of the application. The process starts with ensuring that the filter's current and voltage ratings are compatible with the device's operating conditions. It is noted that the steady state current rating is not the only current rating to consider. Often a filter must be able to withstand the systems full short circuit current rating (SCR) for a specified duration. The suppression levels, measured by the filter's insertion loss, should align with the required levels for effective noise mitigation. It is also important to consider the frequency range of the interference, as the filter must be capable of attenuating noise within this spectrum. The type of filter, whether it be common-mode, differential-mode, pi-filter, low pass, high pass or band pass all depends on the nature of the interference and the application.

The choice between different types of EMI filters, such as differential mode, common mode, or PI filters, depends on the nature of the noise source and the specific filtering requirements of the application. Differential mode filters are designed to attenuate noise that is present between the line and neutral conductors, typically generated by equipment high clock or processor speeds, or other fast-switching electronic components. Electromagnetic reflections in circuit conductors resulting from impedance mis-matches can also generate strong differential currents. On the other hand, common mode filters are used to address noise that is present between both the line and neutral conductors and ground. This type of noise is usually generated by electromagnetic interference from external sources, such as radio frequency interference or electromagnetic pulses, and can also be caused by ground loops, long cable runs, or imbalances in the electrical system. Switching transients in power conversion networks can introduce both differential mode and common mode noise.

PI filters, which consist of a series element (usually inductive) and two shunt elements (usually capacitive), are used when both differential and common mode noise need to be attenuated. They are effective in providing a broad range of filtering and are often used in applications where the noise environment is complex and contains both types of noise.

Once the exact type of filter and its necessary electrical characteristics have been established, one must consider the physical characteristics of the filter, such as size, mounting style, and terminal configuration. Other considerations include environmental performance (acceptable operational temperature and humidity ratings), third party certifications, and system interactions.

When multiple filters are employed in a system, their interactions can significantly impact overall performance. It is essential to analyze how these filters work together to avoid unintended resonances or reduced effectiveness. In some cases, redundant filtering stages can provide additional suppression and improve reliability, especially in critical applications. If a device already incorporates an internal EMC filter, adding an external filter requires careful consideration. The two filters must be compatible in terms of impedance and frequency response to avoid conflicts. Evaluating the combined performance of internal and external filters is necessary to ensure they complement each other and maintain system integrity.

Engineers often face difficult tradeoffs when selecting EMC filters. Balancing size and performance is a common challenge, as larger filters may offer better suppression but can be difficult to accommodate in compact designs. Similarly, there is a tradeoff between cost and effectiveness (as well as cost and regulatory acceptance), with high-performance filters typically coming at a higher price. Another consideration is the balance between insertion loss and bandwidth; while a high insertion loss provides better noise suppression, it may also attenuate desired signals, requiring a careful balance to maintain signal integrity.

Recent Technilogical Advances in EMI/EMC Filters – Amorphous Core Filters

The evolution of core materials has played a pivotal role in enhancing performance and efficiency. Among these advancements, amorphous core filters have emerged as a superior solution, offering distinct advantages over traditional technologies.

Amorphous core filters are characterized by their use of amorphous metal, a material with a non-crystalline structure. Unlike the crystalline lattice found in conventional ferromagnetic materials, the amorphous structure of these metals lacks long-range order, resulting in unique magnetic properties. amorphous materials do not have this regularly repeating atomic arrangement. While there may be some short-range order, where atoms are arranged in a specific way over short distances, there is no repeating pattern that extends over longer distances. The lack of long-range order in amorphous materials is what gives amorphous core filters their unique advantages, such as high permeability and low core loss at high frequencies. Additionally, amorphous core filters are effective over a broad range of frequencies, making them versatile for various applications. Their high permeability and low loss also allow for a compact design, making them smaller and lighter than traditional counterparts without compromising performance.

Traditional EMI filter cores are typically made from materials like silicon steel, ferrite, or powdered iron. Silicon steel, while cost-effective and widely used, suffers from high core losses at higher frequencies, making it less suitable for applications requiring efficient EMI suppression in this range. Ferrite cores offer good high-frequency performance but have lower saturation flux density compared to amorphous metals, which can limit their effectiveness in high-power applications. Powdered iron cores are versatile and provide good frequency response, but they typically have higher losses than amorphous cores at higher frequencies.

TDK-Lambda offers a wide range of EMI filters from DC input to AC input with single and three phase input for medical and industrial applications including high performance amorphous core filters.

www.us.lambda.tdk.com/applications/emi-solutions

Ideal Diodes in small TSSPs

Nexperia has introduced two ideal power diode ICs. The NID5100 is suitable for standard industrial and consumer applications while the NID5100-Q100 has been qualified for use in automotive appli-

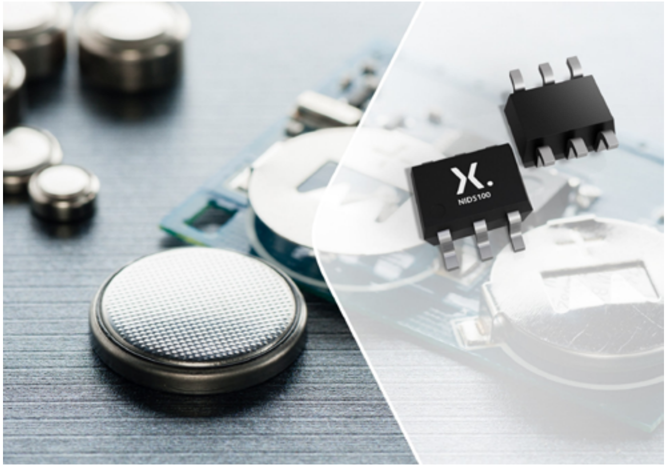

cations. Ideal diodes are MOSFET-based devices that offer much lower forward voltage drop than traditional diodes and make a good replacement option to standard diodes in systems where power efficiency is paramount. The NID5100 and NID5100-Q100 ideal diodes are available in small TSSP6/SOT363-2 leaded plastic packages measuring 2.1 mm x 1.25 mm x 0.95 mm. Applications that can benefit from their electrical performance include smart meters, fire/security sensors, battery powered wearables, and automotive telematics units. The NID5100 is a PMOS based ideal diode where the gate voltage of an internal MOSFET regulates the anode-to-cathode voltage to be eight to ten times lower than the forward voltage drop of similarly rated Schottky diodes. Besides the low forward drop, the MOSFET-based ideal diode also helps to reduce reverse DC leakage current by up to 100 times compared to a typical Schottky diode. The NID5100 supports "OR-ing" multiple power supplies while retaining reverse polarity protection and provides ultra-fast response time for smooth power transfer. Its forward regulation voltage is 31 mV with forward currents up to 1.5 A.

www.nexperia.com

Dual 5 A Low-Side MOSFET Gate Drivers for High-Frequency Applications

Littlefuse launched the IX4341 and IX4342 dual 5 A low-side MOSFET gate drivers, which complete the existing IX434x driver series by adding the remaining two logic input versions. The IX434x series now consists of dual non-inverting, dual inverting, and non-inverting and inverting input versions. The IX4341 and IX4342 drivers' propagation delay times of 16 ns and rise and fall times of 7 ns make them suited for high-frequency applications. Additionally, for higher current requirements, electronics designers can parallel the two channels of the IX4340 and IX4341 devices to form a single 10 A driver. Another feature of the IX434x driv-

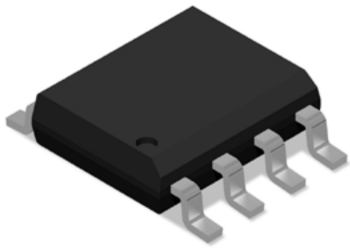

ers is their compatibility with TTL and CMOS logic inputs, enabling direct interfacing with most controllers. Furthermore, each output has an independent ENABLE function and under-voltage lockout circuitry (UVLO). In case of eventual insufficient supply voltage, the gate driver output is asserted low, turning the external power device off.

The devices find applications in various markets, including general industrial and electrical equipment, appliances, building solutions, data centers, energy storage, and renewable energy – whenever MOSFETs in industrial applications such as switch-mode power supplies, DC-DC converters, motor controllers and power converters need to be driven. In terms of packaging a standard 8-pin SOIC, thermally enhanced 8-pin SOIC, and 3×3 mm² MSOP packages are available.

www.littlefuse.com

Evaluation Board for 240 W PD 3.1 Charger with Efficiency >95 %

Eggtronic has unveiled an evaluation board (EVB) that allows engineers to speed the development and significantly reduce the size and cost of 240 W power delivery (PD) 3.1 applications while supporting ultra-fast charging through high efficiency. The SmartEgg 240W PD 3.1 EVB has a peak efficiency above 95% and operates at over 90% efficiency from light load to full load. A single stage that combines zero voltage switching (ZVS) power factor correction (PFC) and quasi-forward isolated regulation significantly reduces bill of materials (BOM) and size of key components (including storage capacitors and magnetics) compared to traditional PFC+LLC and PFC+Asymmetric Half-Bridge (AHB) architectures. The result is a platform that delivers light-load energy savings of up to 50%, achieves a power density of 1.34W/cm^3 (21.9W/in^3) to support extremely compact charger designs and, most importantly, reduces BOM cost. Based on Eggtronic's SmartEgg AC/DC architecture, the EVB incorporates proprietary mixed-signal, low-power EPIC (Eggtronic Power Integrated Controller) 2.0 IC controllers and features built-in protection against overpower, overvoltage, overtemperature, short circuits and brownouts. EPIC, which is based on a 32-bit RISC-V core and a set of high-performance digital and analog

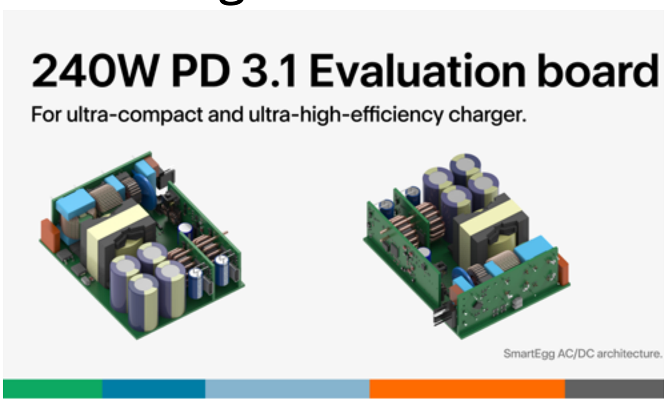

peripherals, incorporates an internal structure that supports multiple independent control loops of both standard and proprietary power conversion architectures. Supplied as a dual-port module, the SmartEgg 240W PD 3.1 EVB can be directly modified for any number of charging ports thanks to the flexibility of the EPIC 2.0 controller, which supports many slave buck converters, each acting as a standalone port.

www.eggtronic.com

MOSFETs in SMD Package for High Performance Applications

Alpha and Omega Semiconductor has announced Power MOSFETs in LFPAK 5x6 packages for voltages of 40 V (AOLF66412, AOLF66413 and AOLF66417), 60 V (AOLF66610), and 100 V (AOLF66910). The devices are designed to withstand harsh environments while maintaining MOSFET performance in applications such as industrial, server power, telecommunications, and solar, where high reliability is required. The LFPAK packaging enables higher board-level reliability due to key packaging features such as gull-wing leads, which offer a ruggedized solution for board-level environmental stresses. The gull-wing leads also enable optical inspection during PCB manufacturing. Another feature enhancement is the LFPAK's larger copper clip, which improves electrical and thermal performance. Advantages of the large clip include improved current handling capabilities, reduced on-resistance, and better heat dispersion compared to wire bonding. A large clip also has low parasitic inductance, enabling lower spike voltage in switching applications. The devices operate with gate-source voltages of ±20 V at maximum junction temperatures of 175 °C. The drain current @ 25 °C and the maximum $R_{DS(on)}$ both depend on the model ranging from 187

to 294 A or, respectively, 1.5 to 4.7 mΩ at a gate-source voltage of 10 V.

www.aosmd.com

High-Performance Power Module Family

SemiQ has added an S7 package to its QSiC™ family of 1200 V, half-bridge MOSFET and Schottky diode SiC power modules. The parts enhance design flexibility for power engineers by providing compact, high-efficiency, high-performance options for new de-

signs while supporting drop-in-replacement in legacy systems that require more efficient operation. This latest announcement sees the availability of a 529A MOSFET module (GCMX003A120S7B1: R_{dsOn} 3.0 mΩ, B1 package), a 348A MOSFET module (GCMX-005A120S7B1: R_{dsOn} 4,9 mΩ, B1 package), and two low-noise SiC Schottky diode half-bridge modules (GHXS300A120S7D5 for 300 A and GHXS400A120S7D5 for 400 A) in an S7 package with industry-standard 62.0 mm footprints and a height of 17.0 mm. The package addresses the size, weight and power requirements of demanding applications ranging from induction heaters, welding equipment and uninterruptible power supplies (UPS) to photovoltaic and wind inverters, energy storage systems, high-voltage DC-DC converters and battery charging systems for electric vehicles (EVs). To guarantee a stable gate threshold voltage and premium gate oxide quality for each module, SemiQ conducts gate burn-in testing at the wafer level and performs various stress. All parts have undergone testing surpassing 1400 V.

www.semiq.com

240 V/1 kA Bidirectional Power TVS Diode in a Surface Mount Package

Bourns has introduced "the industry's first 240 V/1 kA Bidirectional Power TVS (PTVS) Diode that offers the highest power density available in a surface mount package". The PTVS1-240C-M PTVS Diode offers 1 kA surge handling capability under 8/20 µs test conditions and is thus suited for a broad variety of systems that employ high-voltage DC bus architectures. These systems commonly experience high current switching transients and dynamic load behaviors where snubbing is needed, or protection of bus-powered subsystems is required. The PTVS1-240C-M PTVS Diode is a low-leakage device consuming 10 µA in standby while delivering a maximum breakdown voltage of 295 V, repetitive standoff voltage of 240 V and precise clamping voltage of 340 V. Under 10/350 µs conditions, this device is rated for 200 A peak current, and its voltage breakdown sensitivity over temperature shows a linearity of 0.1 %/°C. The company reports that the "surface mount package offers a significant reduced PCB footprint and lower inductance design advantages compared to traditional through-hole mounted Power TVS Diodes". Applications that can benefit from the features and capabilities of the Model PTVS1-240C-M include industrial power

systems, motor controllers and inverters, solar inverters, battery energy storage systems, and factory automation. The device is UL497B certified and meets IEC 61000-4-5 standard specifications. It is also RoHS compliant and halogen free.

www.bourns.com

Electric Vehicle Charger Reference Designs

To accelerate the time to market of an EV charger, Microchip Technology now offers three flexible and scalable EV Charger Reference Designs including a Single-Phase AC Residential, a Three-Phase AC Commercial (up to 22 kW) with Open Charge Point Protocol (OCPP) and System-on-Chip (SoC) and a Three-Phase AC Commercial with OCPP and Display. Most of the active components for the EV charger reference designs are available from Microchip, including the microcontroller (MCU), analog front-end, memory, connectivity and power conversion. This significantly streamlines the integration process, enabling manufacturers to speed time to market for new charging solutions. These reference designs offer complete hardware design files and source code with software stacks that are tested and compliant to communication protocols, including OCPP. OCPP offers manufacturers a standard protocol to communicate between the charge point or charging station and a central system. This protocol is designed to enable interoperability of the charging applications regardless of the network or vendor. The EV Reference Designs are supported by MPLAB X Integrated Development Environment (IDE) to help designers minimize development time, as well as MPLAB Harmony v3 and MPLAB Code Configurator.

www.microchip.com

2" x 4" 250 W Medical and Industrial Power Supply Series

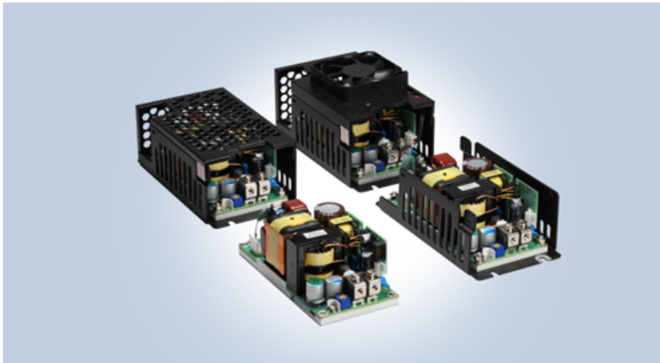

TDK announces additional output voltage models to the 250 W rated TDK-Lambda brand CUS250M series of power supplies in the industry standard 2" x 4" footprint. The full range now covers 12 V, 15 V, 18 V, 24 V, 28 V, 36 V and 48 V and is certified to the IEC 62368-1 and IEC 60601-1 safety standards for industrial and medical applications. This includes both Class I and Class II (no earth ground required) installations. The CUS250M has mechanical configurations that enable convection and/or conduction cooling through the product's baseplate to provide silent cooling. Applications include medical, home healthcare, dental, test, measurement, broadcast, professional audio and industrial equipment. The output can be adjusted to accommodate non-standard voltages, either by the factory or using the on-board potentiometer. The CUS250M operates across an 85 to 264 VAC input and has a earth leakage current of less than 150 µA - including all tolerances. The touch current is <10 µA (Class I) and <70 µA (Class II). In ambient temperatures of -20 °C to +45 °C the CUS250M can deliver up to 250 W conduction cooled without external air. With appropriate derating, operation at up to +80 °C is also possible. The efficiency is up to 94%, and the average efficiency, measured at 25, 50, 75 and 100% loads, is greater than 91%, while offload power consumption is less than 0.5 W when the output is inhibited.

www.jp.lambda.tdk.com

Industrial AC/DC Power Supplies in 2" x 3" Packages

Traco Power released its TXO family of 45, 60 & 120 W compact AC/DC Power supplies. These are the first 3 power levels of a TXO family of power supplies that will eventually go to 500 W. The TXO

line specifically focuses on providing cost-efficient industrial power supplies. Efficiencies of up to 92 % allow for a compact design, and these models are designed to meet the ErP directive (< 0.3 W no load power consumption). Features include an internal EN55032 class B filter, as well as EMC characteristics dedicated for applications in industrial/automation and test & measurement fields. Basic features include a 2" x 3" open-frame construction, a universal input range of 85 – 264 VAC, 3000 VAC reinforced I/O isolation, an internal EN55032 class B filter, short circuit and overvoltage protection, IEC/EN/UL 62368-1 safety approvals and EN 61000-3-2 compliance. The TXO 45/60 series operates at full load convection cooled in the range of -20 °C to +50 °C, while the TXO 120 series operates as follows: 100 W convection / 120 W forced air -20 °C to +50 °C.

www.tracopower.com

Intelligent Power Module for Industrial Motors up to 4 kW

Infineon Technologies expands its 7th generation TRENCHSTOP™ IGBT7 product family with the CIPOS™ Maxi Intelligent Power Module (IPM) series for low-power motor drives. The IM12BxxxC1 series is based on the TRENCHSTOP IGBT7 1200 V and rapid diode EmCon 7 technology. Thanks to the latest micro-pattern trench design, it offers exceptional control and performance. This results in significant loss reduction, increased efficiency, and higher power density. The portfolio includes three new products in variants ranging from 10 A to 20 A for power ratings of up to 4.0 kW: IM-

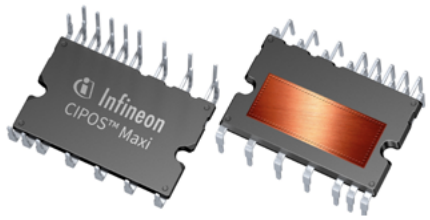

12B10CC1, IM12B15CC1 and IM12B20EC1. The IM12BxxxC1 series is packaged in a DIP 36x23D housing. It integrates various power and control components. This makes it "the smallest package for 1200 V IPMs with the highest power density and best performance in its class", the company says. The IM12BxxxC1 series is particularly suitable for low-power drives in applications such as motors, pumps, fans, heat pumps and outdoor fans for heating, ventilation, and air conditioning. The IPM series offers an isolated dual-in-line molded housing also meets the EMI and overload protection requirements of demanding designs. In addition to the protection features, the IPM is equipped with an independent UL-certified temperature thermistor.

www.infineon.com

40 V MOSFETs in PDFN 33 Packages

Magnachip Semiconductor released four 40V MXT MV MOSFETs designed in Power Dual Flat No-Lead (PDFN) 33 packages for automotive applications. This package reduces the area by more than

60% and the weight by approximately 75% as compared to 40 V MOSFET products packaged in PDFN56. Among these products, three models - AMDV040N029LVRH, AMDV040N036LVRH, and AMDV040N042LVRH - are distinguished by their gate threshold voltage of 1.8 V. The gate threshold voltage determines the point at which the MOSFET switches from an off-state to an on-state. A lower threshold voltage reduces the energy required to operate the MOSFET, thereby decreasing the overall power consumption of the system. For example, the AMDV040N029LVRH provides a typical/maximum $R_{DS(on)}$ of 3.8 mΩ/5.0 mΩ at V_{GS} = 4.5 V and of 2.5 mΩ / 2.9 mΩ at V_{GS} = 10 V. The typical gate charge Q_g at V_{GS} = 10 V is specified with 30 nC.

www.magnachip.com

Advertising Index

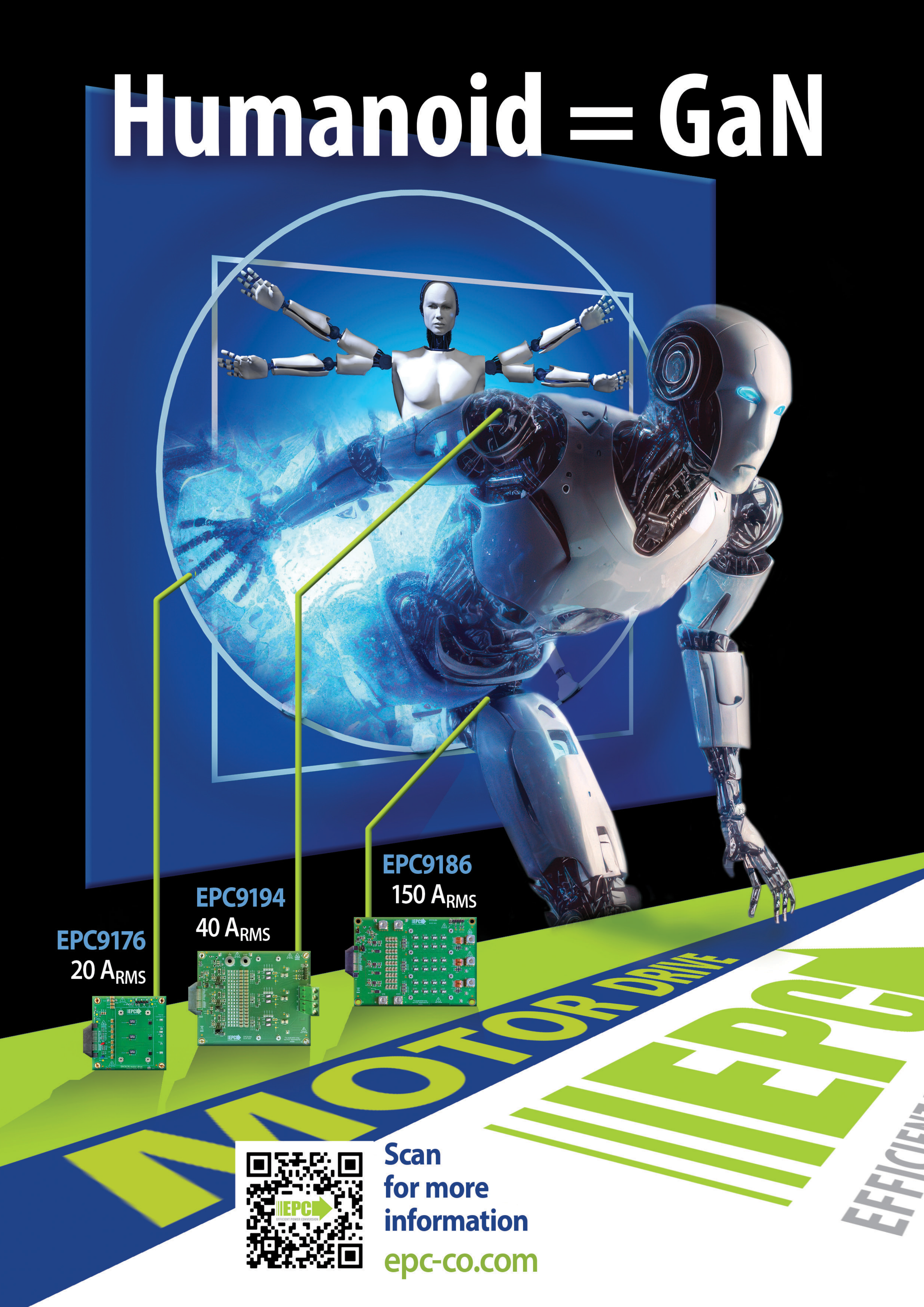
Humanoid = GaN
EPC9186
150 A_RMS
EPC9194
40 A_RMS
EPC9176
20 A_RMS
MOTOR DRIVE
EPC
Scan
for more
information
epc-co.com